

Bayesian Inference for Randomized Benchmarking Protocols

Ian Hincks^{1,2}, Joel J. Wallman^{1,2}, Chris Ferrie³, Chris Granade⁴, and David G. Cory^{5,2,6,7}

¹ Department of Applied Mathematics, University of Waterloo, Waterloo, ON, Canada

² Institute for Quantum Computing, University of Waterloo, Waterloo, ON, Canada

³ Centre for Quantum Software and Information, University of Technology Sydney, Ultimo NSW 2007, Australia

⁴ Quantum Architectures and Computation, Microsoft Research, Redmond, WA 98052, USA

⁵ Department of Chemistry, University of Waterloo, Waterloo, ON, Canada

⁶ Perimeter Institute for Theoretical Physics, Waterloo, Ontario, Canada

⁷ Canadian Institute for Advanced Research, Toronto, ON, Canada

February 2, 2018

Randomized benchmarking (RB) protocols are standard tools for characterizing quantum devices. Prior analyses of RB protocols have not provided a complete method for analyzing realistic data, resulting in a variety of ad-hoc methods. The main confounding factor in rigorously analyzing data from RB protocols is an unknown and noise-dependent distribution of survival probabilities over random sequences. We propose a hierarchical Bayesian method where these survival distributions are modeled as nonparametric Dirichlet process mixtures. Our method infers parameters of interest without additional assumptions about the underlying physical noise process. We show with numerical examples that our method works robustly for both standard and highly pathological error models. Our method also works reliably at low noise levels and with little data because we avoid the asymptotic assumptions of commonly used methods such as least-squares fitting. For example, our method produces a narrow and consistent posterior for the average gate fidelity from ten random sequences per sequence length in the standard RB protocol.

1 Introduction

Accurately characterizing the performance of both large and small quantum devices is vital to ensure that, for example, quantum information processors are reliable and metrology devices are accurate. For critical applications, the reliability of confidence intervals or credible regions for figures of merit is more important than a single-point estimate as there might be practical consequences to over-reporting the performance of a device.

Currently, the only known scalable protocols for characterizing discrete quantum logic gates are randomized benchmarking (RB) [1, 2, 3, 4] and variants thereof, collectively referred to as RB+ (see Table 1 for some variants). The standard RB protocol works by applying random sequences of gates that ideally compose to the identity, where the gates form a unitary 2-design [5]. Measuring in the basis of any initial state after applying a random sequence therefore gives an estimate of the survival probability conditioned upon that random sequence. The survival probability averaged over all random sequences of a fixed length decays exponentially with the length, where the decay rate is a linear function of the average gate fidelity of the overall noise channel. Members of RB+ all have

Ian Hincks: ihincks@uwaterloo.ca

similar structure, modified to suit different goals. RB has been experimentally implemented on a large variety of quantum platforms [6, 7, 8, 9, 10, 11, 12, 13, 14], and is so ubiquitous that its results are often reported with little detail within the context of a larger purpose.

However, these experimental implementations make different ad-hoc statistical assumptions because previous theoretical treatments of RB+ have typically neglected data analysis. The analysis of RB+ experiments is complicated by three factors:

1. every random sequence in a protocol gives rise to a different survival probability, giving rise to a survival distribution for each sequence length;
2. in low- to mid-data regimes, assuming Gaussian errors on either the estimates of the individual survival probabilities or on the mean of the survival distribution through the central limit theorem is dubious; and
3. applying hard physical constraints violates the assumptions of standard statistical fitting routines.

This paper presents a Bayesian data-processing method that overcomes these difficulties, and that can be applied to all members of RB+. As with any Bayesian approach, the output is a joint posterior distribution over all parameters relevant to the problem. Joint distributions over the parameter(s) of interest can be obtained by marginalizing over nuisance parameters, enabling straight-forward statements like ‘under this protocol’s model with this prior knowledge, there is a 95% probability that such-and-such parameter is greater than 0.999’. If a point estimate is required for some parameter, the Bayes estimate is just a sum and division away.

This paper is organized as follows. In [Section 2](#) we layout a notational framework for RB+. In [Section 3](#) we discuss how every protocol relates survival distributions of different lengths through what we call *tying functions*. This leads to the likelihood function of RB+ defined in [Section 4](#), and its necessary dependence on moments of the survival distributions. This is used in [Section 5](#) to define and motivate our main Bayesian model, along with alternative frequentist approaches. We then discuss optimal sequence re-use strategies in [Section 6](#). We present the results of numerical simulations in [Section 7](#). Finally, in [Section 8](#), we briefly discuss how our model can be extended to systems or protocols without strong two-outcome measurements.

2 The Framework of RB+

In this section we provide a general framework to rapidly understand and compare the various protocols related to randomized benchmarking. The framework consists of the following six elements, exemplified in [Table 1](#):

1. \mathbb{G} , Gate Set: the set of R gates $\mathbb{G} = \{G_1, G_2, \dots, G_R\}$ used in the protocol, where this set might satisfy specific conditions such as being a group and a unitary 2-design¹;
2. \mathfrak{E} , Experiment Types: labels for protocols that combine data from multiple sub-protocols, possibly including specification of multiple configurations of preparation and measurement (SPAM), denoted with ρ and E respectively²;
3. M , the Sequence Length: a positive integer, where $\ell(M, e)$ denotes the exact number of gates from \mathbb{G} needed to construct a sequence at length M under experiment type $e \in \mathfrak{E}$;
4. $J_{M,e}$, Allowable Sequences: a discrete distribution whose sample space is the set of gate-indexing tuples $\{1, \dots, R\}^{\ell(M,e)}$, typically uniform on a subset thereof;
5. \vec{x}_T , Tying Parameters: the set of parameters that can be learned from the protocol; and,

¹As a point of practicality, note that gates from \mathbb{G} are often physically implemented by compiling gates from a smaller generating set of gates that need not share any special properties required by \mathbb{G} .

²Rather than including SPAM configurations as experiment types, sometimes protocols may instead compile SPAM configurations into the allowable sequences.

6. *T*, Tying Functions: the known dependence of the parameters on the statistics of the measurement data.

For a given sequence of gate indices $\vec{j} = (j_1, \dots, j_K)$, define the corresponding ideal gate as

$$\mathcal{G}_{\vec{j}} = \mathcal{G}_{j_K} \cdots \mathcal{G}_{j_2} \mathcal{G}_{j_1}, \quad (1)$$

where we use the convention that the scripted version of a letter denoting a unitary operator is the quantum channel which conjugates by that unitary, that is, $\mathcal{G}(\rho) = G\rho G^\dagger$. We write the imperfect implementations of ρ , $\mathcal{G}_{\vec{j}}$, and E as $\tilde{\rho}$, $\tilde{\mathcal{G}}_{\vec{j}}$, and \tilde{E} respectively. The following procedure is then performed experimentally, possibly in a random order to prevent experimental drifts from causing a systematic error:

```

for each sequence length  $M \in \mathbb{M}$  do
  for each experiment type  $e \in \mathfrak{E}_M$  do
    for each sequence  $i = 1, 2, 3, \dots, I$  do
       $\vec{j} \leftarrow \text{RV}(J_{M,e})$ 
       $Q_{M,e,i} \leftarrow \text{RV}\left(\text{Binom}\left(N, \text{Tr}\tilde{E}_e\tilde{\mathcal{G}}_{\vec{j}}(\tilde{\rho}_e)\right)\right)$ 
    end for
  end for
end for

```

where $\mathbb{M} \subset \mathbb{N}$ is some choice of sequence lengths, and (ρ_e, E_e) is the SPAM configuration specified by experiment type e . Here, $\text{RV}(\cdot)$ denotes sampling a random variate from the given distribution, so that $\text{RV}(J_{M,e})$ denotes choosing a random allowable sequence, and $\text{RV}\left(\text{Binom}\left(N, \text{Tr}\tilde{E}_e\tilde{\mathcal{G}}_{\vec{j}}(\tilde{\rho}_e)\right)\right)$ corresponds to repeating this experiment N times and summing the resulting 0s and 1s. This binomial model assumes strong measurement with two outcomes. This condition can be loosened, as discussed in [Section 8](#).

In principle the number of random sequences I can depend on M and e , and the number of repetitions N can depend on M , e , and i , and so on, but we avoid this to maintain subscriptural sanity (though our methods will work nonetheless on such ragged structures). For the same reason, we omit any indices which are not relevant to some specific protocol. Generically, this protocol produces the dataset

$$D = (Q_{M,e,i})_{M \in \mathbb{M}, e \in \mathfrak{E}_M, 1 \leq i \leq I}. \quad (2)$$

As a concrete example, consider standard RB. Then \mathbb{G} is a unitary 2-design which is also a group. There is only one type of experiment for every sequence length, so $\mathfrak{E} = \{0\}$, with a fixed SPAM configuration $E_0, \rho_0 \approx |0\rangle\langle 0|$. We note that our notation allows, however, for formalizing modifications in which two different final measurements are used to decorrelate preparation and measurement errors [\[15\]](#). For sequence length M we require $\ell(M, 0) = M + 1$ gates from \mathbb{G} , where the extra gate corresponds to the final inversion: the allowable sequences at sequence length M are a uniform distribution of all length $M + 1$ gate indices that ideally produce the identity gate, $J_{M,0} = \text{Unif}\left(\{\vec{j} \in \{1, \dots, R\}^{M+1} | \mathcal{G}_{\vec{j}} = \mathbb{I}\}\right)$.

Interleaved randomized benchmarking has a similar structure except, for example, that we may have $\mathfrak{E}_M = \{0, 3\}$, where $e = 0$ represents no interleaving, and $e = 3$ represents interleaving the 3rd gate in \mathbb{G} . As with standard RB, we have $\ell(M, 0) = M + 1$. Interleaved experiments add a fixed gate for every random gate giving us $\ell(M, 3) = 2M + 1$. See [Table 1](#) for more examples of RB+ protocols as described by our framework.

3 Tying functions

The quantity

$$S_{\vec{j},e} = \text{Tr}\tilde{E}_e\tilde{\mathcal{G}}_{\vec{j}}(\tilde{\rho}_e) \in [0, 1] \quad (3)$$

is called the *survival probability* of the sequence $\vec{j} \sim J_{M,e}$ at sequence length M for experiment type $e \in \mathfrak{E}$. For a specific noise model and any protocol described by the previous section, we can consider the discrete *survival distribution* for sequences of length M and experiment type e given by

$$S_{M,e}(q) = \sum_{\vec{j}} \Pr(\vec{j}) \delta(q - S_{\vec{j},e}) \quad (4)$$

where $\delta(\cdot)$ is the delta mass distribution centered at 0, the sum is over all sequences of the right length, $\vec{j} \in \{1, \dots, R\}^{\ell(M,e)}$, and $\Pr(\vec{j})$ is the probability of picking sequence \vec{j} according to the protocol. This distribution has support lying in the unit interval $[0, 1]$.

Such survival distributions depend heavily on the noise model. Complications to the noise model can be introduced successively. See Epstein et al. [16] for a wide set of examples, or Ball et al. [17] for simulations of non-Markovian noise model survival distributions in particular. Letting $\mathcal{E}_{(\cdot)}$ denote a CPTP noise channel and $\vec{j} = (j_1, \dots, j_K)$ a specific gate sequence, starting with the simplest, the broad categories of noise models are

- Gate-independent noise: For every $\mathcal{G}_r \in \mathbb{G}$ we have $\tilde{\mathcal{G}}_r = \mathcal{E}\mathcal{G}_r$ so that $\tilde{\mathcal{G}}_{\vec{j}} = \mathcal{E}\mathcal{G}_{j_K} \cdots \mathcal{E}\mathcal{G}_{j_1}$.
- Gate-dependent noise: For every $\mathcal{G}_r \in \mathbb{G}$ we have $\tilde{\mathcal{G}}_r = \mathcal{E}_r\mathcal{G}_r$ so that $\tilde{\mathcal{G}}_{\vec{j}} = \mathcal{E}_{j_K}\mathcal{G}_{j_K} \cdots \mathcal{E}_{j_1}\mathcal{G}_{j_1}$.
- Gate- and position- dependent noise: For $\mathcal{G}_r \in \mathbb{G}$ appearing at time k we have $\tilde{\mathcal{G}}_r = \mathcal{E}_{r,k}\mathcal{G}_r$ so that $\tilde{\mathcal{G}}_{\vec{j}} = \mathcal{E}_{K,j_K}\mathcal{G}_{j_K} \cdots \mathcal{E}_{1,j_1}\mathcal{G}_{j_1}$.

We can fine-grain these categories further by specifying the types of channels the errors \mathcal{E} can take, for example, depolarizing, extremal, or unitary rotations. We can also, as a matter of preference, move gate noise to the right side of the ideal operator, or consider both left and right noise. Non-markovian noise models obeying causality are also reasonable to study,

- Non-markovian gate dependent noise: For every $\mathcal{G}_r \in \mathbb{G}$ we have $\tilde{\mathcal{G}}_r = \mathcal{E}\mathcal{G}_r$ where \mathcal{E} depends on both r and the gates preceding \mathcal{G}_r , so that $\tilde{\mathcal{G}}_{\vec{j}} = \mathcal{E}_{j_1, \dots, j_K}\mathcal{G}_{j_K} \cdots \mathcal{E}_{j_2, j_1}\mathcal{G}_{j_2}\mathcal{E}_{j_1}\mathcal{G}_{j_1}$.

The set of allowable sequences $J_{M,e}$ typically grows exponentially with the sequence length M , and numerical evidence suggests that it is reasonable to approximate the survival distribution by a continuous distribution.

RB+ protocols have the shared property of *tying together moments of survival distributions* to extract parameters of interest. For example, the gate-independent noise model ties the first moments of RB survivals distributions through the relationship³

$$\mathbb{E}_{S_M}[q] = (A - B)p^M + B \quad (5)$$

where the average gate fidelity of the error map \mathcal{E} is $p + (1-p)/d$, $A = \text{Tr} \tilde{E}_0 \mathcal{E}(\tilde{\rho}_0)$, and $B = \text{Tr} \tilde{E}_0 \mathcal{E}(\mathbb{I}/d)$. Note that we have chosen a slightly different parameterization than that of Magesan *et al.* [4], such that the range of valid SPAM parameters is given by $(A, B) \in [0, 1]^2$.

More generally, every protocol will have a function T which ties together the t^{th} moments of the survival distributions through

$$\mathbb{E}_{S_{M,e}}[q^t] = T(t, M, e, \vec{x}_T). \quad (6)$$

for some subset of all moments. We call T the *tying function*. Here, \vec{x}_T is a vector of parameters required by the tying function, for instance, $\vec{x}_T = (p, A, B)$ in the case of standard RB. As of this writing, the unitarity protocol is the only protocol which ties together moments past the first [18].

³Recall that we omit some indices, here in $S_{M,e}$, for notational convenience. In this case because there is only one experiment type and SPAM setting. Also, the notation $\mathbb{E}_{S_M}[q]$ is the expectation value of the random variable (arbitrarily called q) drawn according to the distribution defined by S_M in Equation 4.

Protocol	Parameter	Symbol	Value
RB [4, 19]	Gate Set	\mathbb{G}	Group and unitary 2-design, R members
	Experiment Types	\mathfrak{E}	$\mathfrak{E}_M = \{0\}$ with SPAM $\rho_0, E_0 \approx 0\rangle\langle 0 $
	Allowable Sequences	$J_{M,e}$	$\text{Unif}(\{\vec{j} \in \{1, \dots, R\}^{M+1} \mathcal{G}_{\vec{j}} = \mathbb{I}\})$
	Tying Parameters	\vec{x}_T	(p, A, B)
	Tying Functions	T	$T(1, M, e, \vec{x}_T) = (A - B)p^M + B$
Interleaved RB [20]	Gate Set	\mathbb{G}	Group and unitary 2-design, R members
	Experiment Types	\mathfrak{E}	$\mathfrak{E}_M = \{0, r\}$ for some $1 \leq r \leq \mathbb{G} $, with SPAM $\rho_e, E_e \approx 0\rangle\langle 0 $
	Allowable Sequences	$J_{M,e}$	$J_{M,0} = \text{Unif}(\{\vec{j} \in \{1, \dots, R\}^{M+1} \mathcal{G}_{\vec{j}} = \mathbb{I}\})$ $J_{M,r} = \text{Unif}(\{\vec{j} \in \{1, \dots, R\}^{2M+1} \mathcal{G}_{\vec{j}} = \mathbb{I}, \vec{j}_{\text{even}} = r\})$
	Tying Parameters	\vec{x}_T	(p_0, p_r, A, B)
	Tying Functions	T	$T(1, M, e, \vec{x}_T) = (A - B)p_e^M + B$
Unitarity [18]	Gate Set	\mathbb{G}	Group and unitary 2-design, R members
	Experiment Types	\mathfrak{E}	$\mathfrak{E}_M = \{0\}$ with SPAM $\rho_0, E_0 \approx 0\rangle\langle 0 $
	Allowable Sequences	$J_{M,e}$	$\text{Unif}(\{1, \dots, R\}^M)$
	Tying Parameters	\vec{x}_T	(u, A, B)
	Tying Functions	T	$T(2, M, \vec{x}_T) = A + Bu^{M-1}$
Leakage RB [21]	Gate Set	\mathbb{G}	Group and unitary 2-design with R members acting on \mathcal{X}_1 , $\mathcal{X} = \mathcal{X}_1 \oplus \mathcal{X}_2$ with $\dim \mathcal{X} = d_1 + d_2$
	Experiment Types	\mathfrak{E}	$\mathfrak{E}_M = \{0, \dots, d_1 - 1\}$ with SPAM $E_e \approx e\rangle\langle e , \rho_e \approx 0\rangle\langle 0 $
	Allowable Sequences	$J_{M,e}$	$\text{Unif}(\{\vec{j} \in \{1, \dots, R\}^{M+1} \mathcal{G}_{\vec{j}} = \mathbb{I}\})$
	Tying Parameters	\vec{x}_T	$(L_1, L_2, \mu_1, p_l, \{A_e\}_{e \in \mathfrak{E}}, \{B_e\}_{e \in \mathfrak{E}}, \{C_e\}_{e \in \mathfrak{E}})$
	Tying Functions	T	$T(1, M, e, \vec{x}_T) = (L_2 A_e + L_1 B_e) / (L_1 + L_2)$ $+ \left(\frac{L_1}{L_1 + L_2} - p_l \right) (A_e - B_e) (1 - L_1 - L_2)^M$ $+ (1 - p_l) (C_e - A_e) (\mu_1 (1 - L_1))^M$
Dihedral Benchmarking [22]	Gate Set	\mathbb{G}	$\langle Z_j = e^{i\pi Z/j}, X \rangle \subseteq \text{SU}(2)$ for some $j \in \mathbb{N}$, R total members
	Experiment Types	\mathfrak{E}	$\mathfrak{E}_M = \{X, Z\}$ with SPAM $E_e, \rho_e \approx (I + e)/2$
	Allowable Sequences	$J_{M,e}$	$\text{Unif}(\{\vec{j} \in \{1, \dots, R\}^{M+1} \mathcal{G}_{\vec{j}} \in \{I, e\}\})$
	Tying Parameters	\vec{x}_T	(p_X, p_Z, A, B_X, B_Z)
	Tying Functions	T	$T(1, M, e, \vec{x}_T) = A + B_e p_e^M$

Table 1: Description of some RB+ protocols within our framework.

4 The Likelihood Function

Let's start with the standard RB protocol in what is known as the 0th order model, as written in Equation 5. The parameter of interest is p since it is related to the average gate fidelity of the average error map. Given a dataset D , as defined in Equation 2, we are interested in inferring the value of p , with A and B treated as nuisances.

Any inference starts with writing down the likelihood function of the parameter of interest [23], along with nuisance parameters, conditioned on the collected data. The total likelihood will be a product over all sequences lengths and sequence draws. Consider just the factor for the i th draw of length- M , resulting in the binomial outcome $d = Q_{M,e,i} \in \{0, \dots, N\}$. The likelihood of this outcome, conditional on drawing the particular sequence \vec{j} , is given by

$$L(p, A, B | d, \vec{j}) = \binom{N}{d} q^d (1 - q)^{N-d} \quad (7)$$

where $q = S_{\vec{j}}$ is the survival probability of sequence \vec{j} . The conditional is removed by marginalizing q over the survival distribution,

$$L(p, A, B | d, M) = \mathbb{E}_{S_M} \left[\binom{N}{d} q^d (1 - q)^{N-d} \right]. \quad (8)$$

At this point we have run into a very serious problem. This expression cannot be simplified, even in principle, unless we know more about the survival distribution S_M . There is one exception, however, first explicitly pointed out in an appendix of Granade et al. [24]: if $N = 1$, then the expectation’s integrand is linear in q for both values of d and so only the first moment of S_M matters; we get

$$L(p, A, B|d = 1, M) = (A - B)p^M + B \tag{9}$$

for standard RB, or more generally,

$$L(\vec{x}_T|d = 1, M, e) = T(1, M, e, \vec{x}_T) \tag{10}$$

for any protocol whose first moments are tied together. This fact was exploited to great effect by those authors. The same argument shows that the first N moments of $S_{M,e}$ are potentially relevant to the likelihood function for any protocol, and therefore some characterization of them should be appended to the list of nuisance parameters.

Alternatively, one might argue to simply enforce the constraint $N = 1$. This is a reasonable suggestion, and is explored in Section 6 where it is shown that $N = 1$ should be considered best-practice for protocols which only tie together their first moments, and whose implementations are quick at switching between random sequences. For some experimental setups, however, switching the sequence every experiment would dominate the duty cycle. The way around this is through fast logic near the quantum system [25], such as was recently demonstrated by Heeres *et al.* [14] in the case of a transmon qubit coupled to an oscillator-encoded logical qubit. Or perhaps, even more seriously, some systems are not capable of strong measurement, and so a binomial model with $N = 1$ is not physically possible. In this case we can still write down a likelihood function, no longer conditionally binomial as seen in Section 8, but one that will involve higher moments by necessity. Finally, in some cases, the second moment is the moment of interest, as in the unitarity protocol, so that $N = 1$ is completely insensitive to the quantity of interest.

In any case, a great deal of RB+ experiments have been performed with $N > 1$ and so it behooves us to devise a statistically rigorous approach for analysing such data.

5 Constructing Agnostic Models

In the last section we noted that for a repetition value of N , to fully specify the likelihood function of an RB or related protocol, we require at least N parameters per sequence length and experiment type, in addition to the parameters of the tying function. These extra parameters correspond to moments of the survival distributions. We will write \vec{x}_S to denote these new parameters, whatever they end up being, distinguishing them from the parameters of the tying function, \vec{x}_T . One must tread carefully in any analysis that follows this observation. The goal of this section to develop a framework where we treat these nuisance parameters in a principled yet practical way, while at the same time remaining as agnostic about their structure as possible.

5.1 Parameterizations

A Bayesian, by instinct, may be tempted to throw all of the unknown moments of the survival distributions into an inference engine as nuisance hyperparameters. In principle there is nothing wrong with this. However, it would lead to a huge number of parameters for even modest values of N . Care would be required in restricting the domains of these moments, for example, the variance σ^2 of a distribution with support on $[0, 1]$ and expectation value μ must always satisfy $0 \leq \sigma^2 \leq \mu(1 - \mu)$.

One might suggest next to truncate the number of moments to be included as hyperparameters down to some tractable, empirically motivated constant. But even in this case, one must specify the higher moments somehow. For example, one might choose to set them all to zero. This would effectively restrict the space of allowed survival distributions to some strange, unmotivated family of

distributions. Instead, one might make the moments above the truncation cutoff sure functions of those below in some sensible way.

At this point, we have basically argued for the use of parameterized families of probability distributions; any family of probability distributions, like the Gaussian or gamma families, can be defined as a rule that specifies all moments of a given member in terms of a few parameters. For us, the most natural starting point is the beta distribution family. This family is conjugate to the binomial distribution, and is the canonical family of continuous distributions with support on the unit interval. A member with parameters $\alpha, \beta > 0$ is written $\text{Beta}(\alpha, \beta)$, and has a density function defined by

$$\text{pdf}_{\text{Beta}}(q) = \frac{q^{\alpha-1}(1-q)^{\beta-1}}{\text{B}(\alpha, \beta)} \quad (11)$$

where the normalization constant $\text{B}(\alpha, \beta)$ is the beta function. Its first and second central moments are given by $\mu = \frac{\alpha}{\alpha+\beta}$ and $\sigma^2 = \frac{\alpha\beta}{(\alpha+\beta)^2(\alpha+\beta+1)}$, respectively. These equations can be uniquely inverted as

$$\alpha = \mu^2(1-\mu)/\sigma^2 - \mu \quad (12a)$$

$$\beta = \mu(1-\mu)^2/\sigma^2 - (1-\mu), \quad (12b)$$

which provides an alternate parameterization of the family. In a slight abuse of notation, we write $\text{Beta}(\mu, \sigma)$ for a member written in the new coordinates. Alternate parameterizations and their transforms are provided in [Section D](#), and we similarly abuse notation for these other coordinates, writing, for example, $\text{Beta}(\mu, r)$ where $\sigma^2 = r\mu^2(1-\mu)^2$.

This family can produce quite a wide variety of shapes even though it only has two parameters. Setting $\alpha = \beta = 1$ results in the uniform distribution on $[0, 1]$. Fixing any mean $\frac{\alpha}{\alpha+\beta} \in (0, 1)$ while increasing α and β decreases the variance, and the distribution approaches a normal shape. On the other hand, decreasing α and β while the mean is kept fixed increases the variance toward $\mu(1-\mu)$; the probability density at first spreads out over the whole interval $[0, 1]$, and when this is no longer able to keep increasing the variance, the mass begins to build up at the end points, approaching a weighted mixture of two delta functions.

Using this family, for a first order tying function, every sequence length, experiment type, and measurement operator would add one parameter to the likelihood model, so that $\vec{x}_S = \{\sigma_{M,e}\}_{M \in \mathcal{M}, e \in \mathbf{e}_M}$, or some other parameterization thereof. In the case of any protocol which ties together only first moments, we get the hierarchical model

$$\vec{x}_T \sim \pi(\vec{x}_T) \quad (13a)$$

$$\mu_{M,e} | \vec{x}_T = T(1, M, e, \vec{x}_T) \quad (13b)$$

$$\sigma_{M,e} \sim \pi(\sigma_{M,e}) \quad (13c)$$

$$q_{M,e,i} | \mu_{M,e}, \sigma_{M,e} \stackrel{\text{iid}}{\sim} \text{Beta}(\mu_{M,e}, \sigma_{M,e}) \quad (13d)$$

$$Q_{M,e,i} | q_{M,e,i} \stackrel{\text{iid}}{\sim} \text{Binom}(N, q_{M,e,i}) \quad (13e)$$

for the dataset D . The horizontal line is a visual aid to separate the prior from the likelihood distribution, and $\pi(\cdot)$ refers to the prior distribution of the given parameters. The quantities $q_{M,e,i}$ are latent random variables representing survival probabilities — they can be analytically integrated out of the model if desired, resulting in a beta-binomial distribution instead. This set of sampling statements, which are sequentially dependent on previous variables, is an example of a probabilistic program. It is a convenient way of specifying the joint distribution of the prior and the likelihood, which is proportional to the posterior distribution.

Models for higher-order tying functions are just as easy to write down. Note, however, that the beta distribution only has two parameters, so that if both of the first two moments are tied together, there

is no more uncertainty in the survival distributions (conditional on a specific value of \vec{x}_T). This can be solved by using a larger family of distributions, or through a nonparametric approach, as discussed in the following section.

5.2 Nonparameterizations

The assertion that every survival distribution is approximately beta distributed may sometimes be too strong. In this section we would like to loosen this restriction. One viable path is to use a bigger family, such as the generalized beta family with five parameters [26]. Even more generally, we can resort to Bayesian nonparametrics. This is the approach that we take, and in particular, we use Dirichlet process mixtures, which are distributions of distributions⁴.

Let $\text{DP}_K(\alpha, G_0)$ denote a Dirichlet process with a concentration parameter $\alpha > 0$ and a base distribution G_0 that has support on the parameter space Ω , and that is truncated to K modes⁵. We would like to replace the draw of $q_{M,e,i}$ from a beta distribution (see Equation 13) to a draw from a random distribution G , such as $G \sim \text{DP}_K(\alpha, G_0)$. The Dirichlet process has two shortcomings that prevent us from directly using it for this purpose. The first is that its variates are not continuous distributions, and the second is that the moments of its draws are random, whereas we would like the ability to (conditionally) fix some of them according to the tying functions.

To overcome these problems we modify the Dirichlet process into a new nonparametric family that we call *constrained Dirichlet process beta mixtures* (CDPBM), denoted $\text{CDPBM}_K(\alpha, G_0, \cdot)$, whose definition is motivated in Section B.2. In short, if the desired mean value of our random distributions is $0 < \mu_1 < 1$, then the random distribution $G \sim \text{CDPBM}_K(\alpha, G_0, \mu_1)$ is drawn as follows:

$$\sum_{k=1}^K w_k \delta_{(\nu_k^*, r_k)} \sim \text{DP}_K(\alpha, G_0) \quad (14a)$$

$$\nu_k = \frac{1}{1 + e^{-\nu_k^* - h}} \text{ with } h \text{ such that } \sum_{k=1}^K w_k \nu_k = \mu_1 \quad (14b)$$

$$G = \sum_{k=1}^K w_k \text{Beta}(\nu_k, r_k). \quad (14c)$$

Here, the Dirichlet process sample space is $(\nu_k^*, r_k) \in \mathbb{R} \times (0, 1) = \Omega$, upon which the base distribution G_0 is defined, and we are using the (μ, r) parameterization of the beta family (see Section D). This procedure ensures that $\mathbb{E}[G] = \mu_1$, and that the support of G lies within $[0, 1]$. We typically choose $G_0 = \text{N}(0, 1.9) \times \text{Unif}(0, 1)$ as a broad prior, and assign a hyper-prior $\alpha \sim \text{Gam}(1, 1)$.

With this defined, our nonparametric model for analyzing RB+ data is a straight-forward modification of Equation 13, given by

$$\vec{x}_T \sim \pi(\vec{x}_T) \quad (15a)$$

$$\mu_{M,e} | \vec{x}_T = T(1, M, e, \vec{x}_T) \quad (15b)$$

$$\alpha_{M,e} \stackrel{\text{iid}}{\sim} \text{Gam}(1, 1) \quad (15c)$$

$$G_{M,e} | \alpha_{M,e}, \mu_{M,e} \stackrel{\text{ind}}{\sim} \text{CDPBM}_K(\alpha_{M,e}, G_0, \mu_{M,e}) \quad (15d)$$

$$q_{M,e,i} | G_{M,e} \stackrel{\text{ind}}{\sim} G_{M,e} \quad (15e)$$

$$Q_{M,e,i} | q_{M,e,i} \stackrel{\text{ind}}{\sim} \text{Binom}(N, q_{m,i}). \quad (15f)$$

⁴We provide a brief introduction to Dirichlet processes and Dirichlet process mixtures in Section B.1.

⁵As a brief bit of context, recall that G_0 is the mean value of $\text{DP}_K(\alpha, G_0)$, and that α can be interpreted as the number of ‘prior observations’ from samples of $\text{DP}_K(\alpha, G_0)$; it scales inversely with the variance of $\text{DP}_K(\alpha, G_0)$.

A slight modification is needed for protocols which tie together higher moments, which we omit for brevity; see [Section B.2](#).

5.3 Frequentist Approaches

Though we are primarily concerned with a Bayesian approach, we are also interested in comparing to frequentist methods. To date, the *de facto* frequentist inference tool for RB+ data (with exceptions) has been least-squares fitting (LSF) to exponential decay models. Generally, the justification for LSF is that it is equal to the maximum likelihood estimator (MLE) in the case of Gaussian noise on the data.

There are a couple of reasons to be cautious when using estimates and confidence regions based on LSF in the case of RB+. One is that the distribution of the data is not Gaussian, except approximately in the high data regime, and therefore the MLE is not being reported, but some sort of approximation thereof. Another is that weights need to be chosen for weighted LSF (WSLF)—using uniform weights implicitly makes assumptions about the nature of the noise model and should always be avoided.

It is non-trivial to choose appropriate weights for WLSF. One may be tempted to use sample variances as weights, but there is a subtle issue that these variances do not directly represent the uncertainty of the quantities of interest at a given sequence length and experiment type; they partially contain unnecessary weight due to finite sampling statistics. Even if this is corrected for, one must also make sure that weights are assigned consistently. Additionally, one needs a heuristic for assigning a non-zero weight in the case of no variance in the outcomes at a given sequence length of a protocol.

For these reasons our preferred frequentist method for analyzing data from RB+ models containing many sequence lengths is to look directly at the MLE. This can be done by using a likelihood function that assumes that survival distributions are beta distributed—see the second half of [Equation 13](#). The log-likelihood of this model is easily and reliably maximized with gradient-based numerical methods. We avoid having to assign weights at every sequence length since they are now treated as nuisances of the global fit. Confidence intervals for this estimator can be constructed through standard bootstrapping techniques (see for example the survey article of DiCiccio and Efron [\[27\]](#)). In this paper we construct bootstrap distributions of the tying parameters by computing the MLE on random data replications drawn from the empirical (non-parametric) distribution of the data, or by sampling the likelihood distribution at the MLE of the data (parametric). Samples are always drawn on a per-sequence-length basis, so that the shape of the bootstrapped data is the same as that of the original data. Confidence intervals are constructed with the simplest bootstrap- t procedure. That is, we look directly at the CDF of these bootstrap distributions.

Occasionally we will also consider the WLSF for the sake of interest. In such cases, we set weights equal to the sample variances of the binomial data normalized by N . We do this because it has been a popular approach historically.

6 Sequence Re-Use

Thus far we have only talked about data analysis. In this section we discuss which experiments to perform in the first place. Specifically, we address the question of how many times a fixed random sequence from an RB+ protocol should be reused. In [Section 4](#) we hinted at the fact that every random sequence should, ideally, only be used once. Here, we qualify and quantify this idea.

With all of the heavy lifting of getting to the survival distribution out of the way, we can cast the problem of sequence re-use as one of pure statistics. Or, we can think of a concrete and conceptually simple isomorphic problem—we can think of a survival distribution as a bag of coins with different biases. Suppose this bag has a mean bias \bar{q} and a standard deviation of biases σ (or, equivalently characterized by the second moment μ_2). We want to estimate these unknown quantities from selecting coins from the bag, at random, and flipping them. The isomorphism is that the statistical conclusions of flipping the same coin more than once are the same as repeating a given gate sequence in RB.

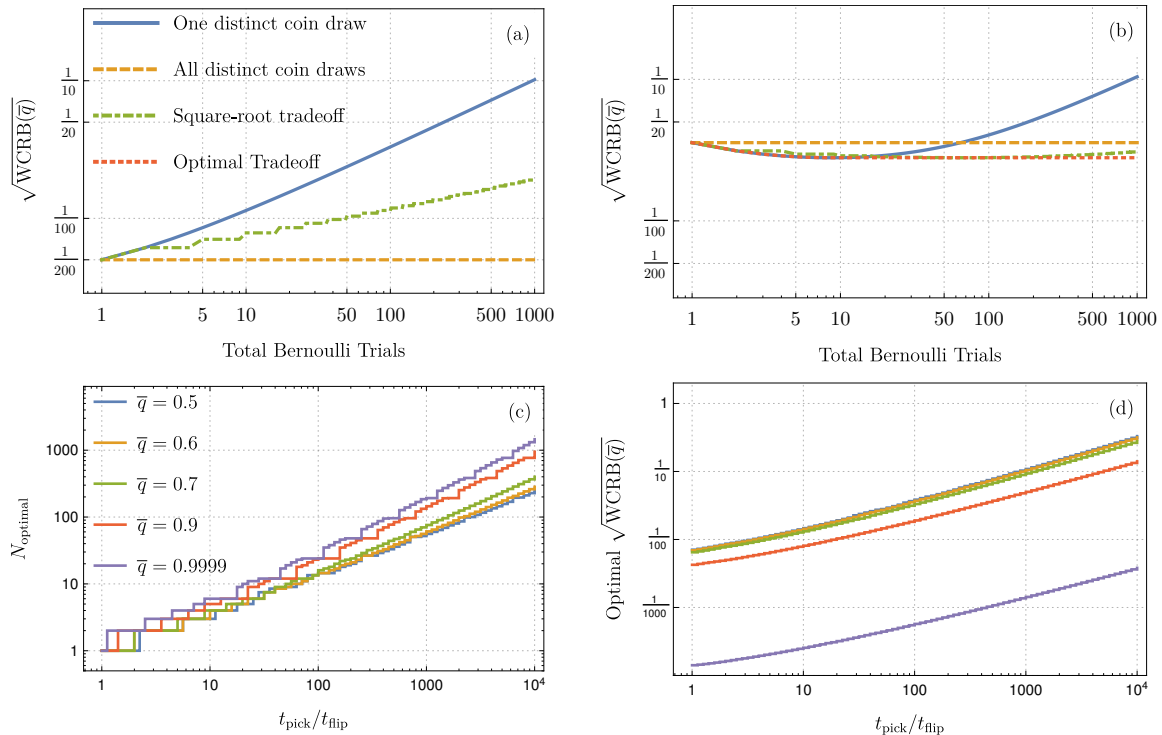


Figure 1: (a-b) Supposing a fixed budget of Bernoulli trials for the bag-of-coins experiment, the WCRB (Equation 19) of the mean coin bias \bar{q} is shown, normalized to the time it takes to complete the full experiment. The true parameters of the bag are $\bar{q} = t = 0.5$, a single coin flip takes $t_{\text{flip}} = 100$ us, and switching coins takes $t_{\text{pick}} = 0$ and $t_{\text{pick}} = 5$ ms = $50t_{\text{flip}}$ for (a) and (b), respectively. We see choosing all coins to be different is no longer the best strategy when $t_{\text{pick}} > 0$. To explore this, in (c-d), given a ratio $t_{\text{pick}}/t_{\text{flip}}$, we compute the optimal number of coin flips N and the resulting optimal WCRB for $t_{\text{flip}} = 100$ us, $t = 0.5$, and various values of \bar{q} . (In these final two plots, there is no longer a fixed budget of trials; global minima were found with respect to N .)

So, by considering the trade-off in the number of repetitions of flips using the same coin versus selecting a new coin, we can understand the optimal experimental design policy in RB.

6.1 First moment estimators

Naturally, we start with the first moment. With protocols that tie only first moments, we only care, by necessity, about inferring values which depend on \bar{q} , but none of the higher moments of the bag. Conditional on picking a coin with bias q , if we perform N Bernoulli trials and add them up, we have the conditional random variable

$$Q|q \sim \text{Binom}(N, p) \quad (16)$$

with conditional cumulants $\mathbb{E}[Q|q] = Np$ and $\text{Var}[Q|q] = Nq(1 - q)$.

This gives $\text{Var}[Q] = N\bar{q}(1 - \bar{q}) + N(N - 1)\sigma^2$ through the law of total variance. If we independently and identically repeat the process of drawing a different coin I times and perform N Bernoulli trials on each, we end up with

$$\text{Var} \left[\sum_{i=1}^I \frac{Q_i}{N \cdot I} \right] = \frac{1}{I} \left(\frac{\bar{q}(1 - \bar{q})}{N} + \frac{N - 1}{N} \sigma^2 \right) \quad (17)$$

as the variance of the scaled quantity $\sum_{i=1}^I Q_i / (N \cdot I)$ whose mean value is \bar{q} . The take-away from this formula is that the variance approaches 0 as we increase the number of coins (sequences) we use, but asymptotes to the finite value σ^2 if we fix I and increase the binomial parameter N (re-use of the same sequence). If we consider instead the total number of flips of all coins to be fixed, $I \cdot N = \text{const.}$, we can see at once that the variance is minimized when $N = 1$ by completely eliminating the contribution from σ .

We have looked at the variance formula above because it has a simple derivation and gets the point across. However, a better quantity to consider is the Fisher information and the resulting Cramér–Rao bound of \bar{q} , because it gives a rigorous bound on how well any (unbiased) estimator of \bar{q} can do. Supposing that we explicitly choose our bag to have a beta distribution with mean value \bar{q} and variance $\sigma^2 = t\bar{q}(1 - \bar{q})$ for some $0 < t < 1$, then our likelihood distribution is Beta-Binom(N, μ, t) and the two-by-two Fisher information matrix, $J(\bar{q}, t)$, is given by the negative expected value of the Hessian of the log-likelihood function. By virtue of our choice of parameterization (\bar{q}, t) , the Fisher information matrix happens to be diagonal, and so the the Cramer-Rao bound reads

$$\text{Var}[\hat{q}] \geq \frac{1}{I \cdot J(\bar{q})} \quad (18)$$

where $J(\bar{q}) = J(\bar{q}, t)_{1,1}$ and $\hat{q}(Q_1, \dots, Q_I)$ is any unbiased estimator of \bar{q} that depends on I iid samples from the likelihood.

So far we have neglected any cost associated with picking a new coin from our analysis, which is the main reason why experimentalists re-use sequences. We can include this cost by considering the Fisher information per unit time, $J(\bar{q})/T$, where T is the time it takes to collect the data. Suppose that it takes time t_{pick} to pick a new coin and time t_{flip} to flip a coin once. Then we have $T = I(t_{\text{pick}} + Nt_{\text{flip}})$, and the CRB weighted by experiment cost is

$$\text{Var}[\hat{q}]/\text{Hz} \geq \frac{(t_{\text{pick}} + Nt_{\text{flip}})}{J(\bar{q})} \equiv \text{WCRB}(\bar{q}) \quad (19)$$

where we have assumed T is in units of seconds. Note that if we take the square root of both sides we get the usual units for sensitivity. This figure of merit is explored in [Figure 1](#).

6.2 Second moment estimators

As before, we draw a coin I times and perform N Bernoulli trials on each. This time, however, we estimate the *second moment* via summing the squares of the number of successes. This estimator is biased, but not asymptotically so:

$$\mathbb{E} \left[\sum_{i=1}^I \frac{Q_i^2}{I \cdot N^2} \right] = \mu_2 + \frac{1}{N}(\bar{q} - \mu_2). \quad (20)$$

That is, as the number of repetitions N increases, this estimator becomes less biased.

Due to this bias, the Cramér–Rao cannot tell us much about this estimator. But, we can directly calculate the mean squared error. As before, though, we consider a fixed total number of measurements $T = N \cdot I = \text{const.}$ and calculate $T \cdot \text{MSE}$.

Since the MSE involves the square of the second moment, we need to calculate

$$\begin{aligned} & \mathbb{E} \left[\left(\sum_{i=1}^I \frac{Q_i^2}{I \cdot N^2} \right)^2 \right] = \frac{1}{I^2 N^4} \sum_{j,k=1}^I \mathbb{E}[Q_j^2 Q_k^2] \\ & = \frac{1}{I^2 N^4} \left(\sum_{k=1}^I \mathbb{E}[Q_k^4] + \sum_{j \neq k=1}^I \mathbb{E}[Q_j^2] \mathbb{E}[Q_k^2] \right) \\ & = \frac{1}{I^2 N^4} (I \mathbb{E}[Q^4] + I(I-1) \mathbb{E}[Q^2]^2). \end{aligned} \quad (21)$$

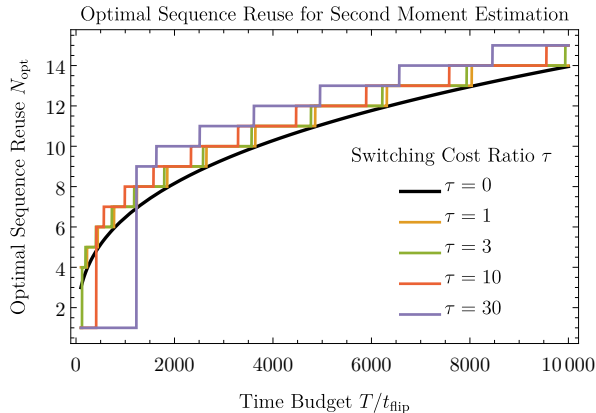


Figure 2: The optimal sequence reuse N_{opt} for second moment estimation (as used, for example, in the unitarity protocol), plotted as a function of the total time budget allowed T , for each of several choices of the switching cost ratio $\tau := t_{\text{pick}}/t_{\text{flip}}$.

The fourth moment of the Beta-Binomial $\text{Beta-Binom}(N, \mu, \mu_2)$ is simple yet still too messy to usefully reproduce here.

We calculate the optimal repetition rate by averaging the total cost over a uniform prior on the domain of validity in the parameterization of (μ, μ_2) . The final answer for the optimal value of N is

$$N_{\text{opt}} = \left(\frac{16}{40 + 32 \ln(2) - 3 \ln(3)} \right)^{\frac{1}{3}} T^{\frac{1}{3}} + O\left(\frac{1}{T^{\frac{1}{3}}}\right), \quad (22)$$

or roughly $0.65T^{\frac{1}{3}}$. A ball-park amount of data usually taken at each sequence length in randomized benchmarking is about a kilobyte. This corresponds to about $N = 13$ repetitions per sequence and $I = 615$ difference sequences.

It is also of interest to consider the case when $\mu \in (l, 1)$ for some lower bound l . For example, suppose we are fairly confident that our fidelity is above 90%. In this case, we still have

$$N = C(l)T^{\frac{1}{3}} + O\left(\frac{1}{T^{\frac{1}{3}}}\right), \quad (23)$$

for some $C(l) < C(0)$. For example, taking $l = 0.9$, we have $N = 0.39T^{\frac{1}{3}}$.

Finally, we generalize the calculation of Equation 22 to include the effects of finite switching costs $\tau := t_{\text{pick}}/t_{\text{flip}}$. In doing so, we proceed numerically, as the series expansion obtained in Equation 22 is much less useful for $\tau > 0$. We plot the results in Figure 2, noting that even for $\tau = 30$, the optimal sequence lengths found do not deviate substantially from the case where there is no switching cost. Thus, $N_{\text{opt}} \approx 0.65T^{\frac{1}{3}}$ remains a useful heuristic in this case, even if it is no longer a rigorous approximation.

7 Numerical Results

In this section we explore our Bayesian model with a collection of numerical examples, using various protocols and error models. Code to reproduce these results can be found online [28].

As with most Bayesian models, analytic formulae for posterior distributions are intractable. Our posterior in the examples throughout this section are therefore computed with numerical techniques. In particular, we use the Hybrid Monte Carlo (HMC) sampler using the No-U-Turns (NUTS) heuristic [29, 30]. This is a type of Markov chain Monte Carlo (MCMC) sampler that has gained widespread use due to its lack of tuning parameters, fast mixing rate, and ability to handle large numbers of parameters. More details about our sampling strategies are outlined in Section A.

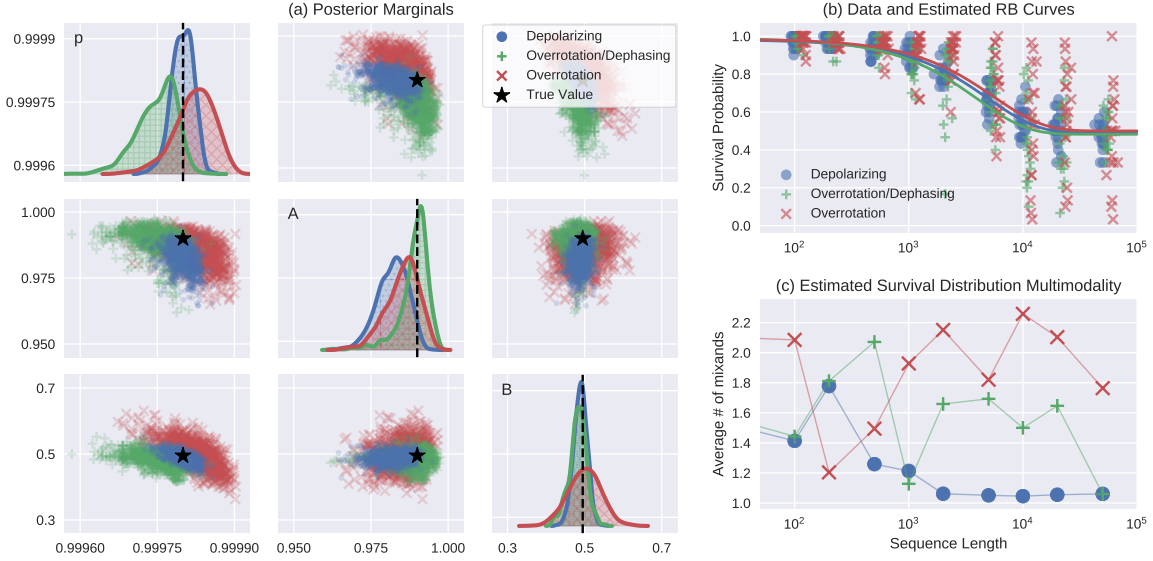


Figure 3: (a) Single and joint posterior marginals of the parameters p , A , and B are shown for each of the three noise models defined in Section 7.1 of the main text for the standard RB protocol. (b) Using Bayes' estimate for these three parameters, the curve $(A - B)p^M + B$ is plotted for each model, displayed on top of the normalized data used in the inference. The unusual shape is due to the log-linear scale, and jitter in the x -axis on the data points was added for visual appeal — for all three models $I = 20$ random sequences were used with $N = 30$ repetitions each at each of the sequence lengths $\mathbb{M} = \{1, 100, 200, 500, 1000, 2000, 5000, 10000, 20000, 50000\}$, where the maximum sequence length is chosen according to the $M_{\max} = 1/(1 - F)$ heuristic [24]. (c) The posterior shown in (a) was calculated using the model in Equation 15, which describes each survival distribution as a mixture of beta distributions, and so finally, we plot the posterior mean of $1/\sum_{k=1}^K w_k^2$ for each survival distribution, where the weights w_k are defined in Equation 14. This quantity ranges between 1 and K and quantifies the estimated number of relevant mixands in each survival distribution. The low values justify our CDPBM truncation at $K = 10$.

7.1 RB with Various Noise Models

As a first example, we consider the standard RB protocol on a qubit under three noise models. We use an order 12 subgroup of the usual 24 member Clifford group as our gateset. This subgroup is still a 2-design and can be generated as $\mathbb{G} = \langle Z, \sqrt{Z}H \rangle$, where $H = \begin{pmatrix} 1 & 1 \\ 1 & -1 \end{pmatrix} / \sqrt{2}$ and $Z = \begin{pmatrix} 1 & 0 \\ 0 & -1 \end{pmatrix}$. Our three noise models are defined as

$$\mathcal{E}_r^1 = \Lambda_{s_1} \quad (24a)$$

$$\mathcal{E}_r^2 = \Phi_{s_2} \circ \Theta[G_r, \epsilon_2] \quad (24b)$$

$$\mathcal{E}_r^3 = \Theta[G_r, \epsilon_3] \quad (24c)$$

where $\tilde{\mathcal{G}}_r = \mathcal{G}_r \circ \mathcal{E}_r^i$ is the actual implementation of the ideal gate \mathcal{G}_r for $r = 1, \dots, R$ and where

$$\Lambda_s(\rho) = (1 - s)\rho + s \text{Tr}[\rho] \mathbb{I}/2 \quad (25a)$$

$$\Phi_s(\rho) = (1 - s)\rho + sZ\rho Z \quad (25b)$$

$$\Theta[U, \epsilon](\rho) = \begin{cases} \rho & U \text{ is some z-rotation} \\ U^\epsilon \rho (U^\epsilon)^\dagger & \text{else} \end{cases} \quad (25c)$$

are the depolarizing, dephasing, and transverse overrotation channels, respectively. Therefore \mathcal{E}_r^1 is a gate independent depolarizing channel, \mathcal{E}_r^2 is gate independent dephasing combined with a gate

dependent overrotation by amount ϵ_2 , and \mathcal{E}_r^3 is purely gate dependent overrotation by amount ϵ_3 . Constants were chosen by trial and error so that all three noise models result in exactly the same RB decay base $p = 0.9998$, ultimately achieved with the choices $s_1 = 0.0002$, $s_2 = 0.000028954$, $\epsilon_2 = 0.01$, and $\epsilon_3 = 0.11132$. A formula for computing p given a gate dependent noise model is provided in Ref. [31].

Data was simulated under each noise model with the initial state $\rho = |0\rangle\langle 0|$ and the measurement $M = 0.99|0\rangle\langle 0|$ at each of the sequence lengths $\mathbb{M} = \{1, 100, 200, 500, 1000, 2000, 5000, 10000, 20000, 50000\}$. At each sequence length, $I = 20$ random sequences were drawn and $N = 30$ repetitions were used for each. To produce histograms of the survival distributions, however, thousands of simulations were done per sequence length.

This dataset was processed in a few different ways. Posterior results using the CDPBM-survival-distribution model Equation 15 are summarized in Figure 3. The slightly simpler Beta-survival-distribution model Equation 13 was also used, which is compared to the CDPBM model in Figure 4, along with weighted least squares fitting, and a non-parametric bootstrap with 2000 samples. Additionally, estimates of the shapes of some survival distributions are seen in Figure 5. The prior distribution on the tying parameters was chosen to be $\pi(p, A, B) = \text{Unif}([0, 1]^3)$ in all cases.

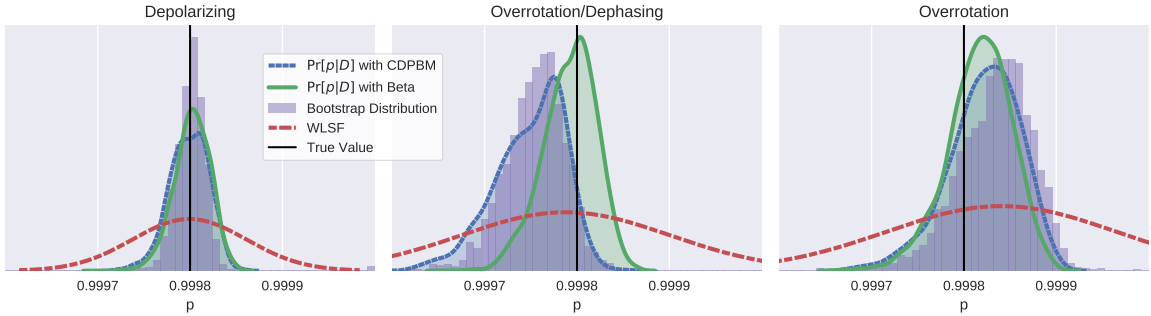


Figure 4: For each of the three noise models defined in Section 7.1, four types of data processing are performed to compare their estimates of (and uncertainties in) the parameter p from the standard RB protocol. Each dataset consists of $I = 20$ random sequences with $N = 30$ repetitions each at each of the sequence lengths 1, 100, 200, 500, 1000, 2000, 5000, 10000, 20000 and 50000. The first two methods show the posterior marginal of p under the models from Equation 15 and Equation 13, respectively. The next two methods are non-parametric bootstrapping and weighted least squares fitting, as described in Section 5.3.

7.2 Low Data Regime

One advantage of using the full likelihood model is that it transitions seamlessly to low data regimes where normal approximations fail and the usual sample moments are ill-defined. At a given sequence length, if we only pick a handful of sequences I with a handful of shots N each, then there is a good chance that $Q_{M,e,i}$ will be equal for all $i = 1, \dots, I$. This is especially true near the boundaries 0 and 1. In this event, it is difficult to use a weighted least-squares fit.

To illustrate our Bayesian model in this regime, we consider simulated data from standard RB using the gate dependent overrotation model from Equation 24c. We choose this model because it has very wide survival distributions, as seen in Figure 5.

We wish to demonstrate that posterior distributions in the low-data regime meaningfully report the parameter of interest, p . The worst thing an inference method can do in this example is predict that the RB parameter p is larger than it actually is. Therefore instead of summarizing a posterior in terms of its mean value (Bayes' estimate), it is more helpful to summarize it in terms of the the value

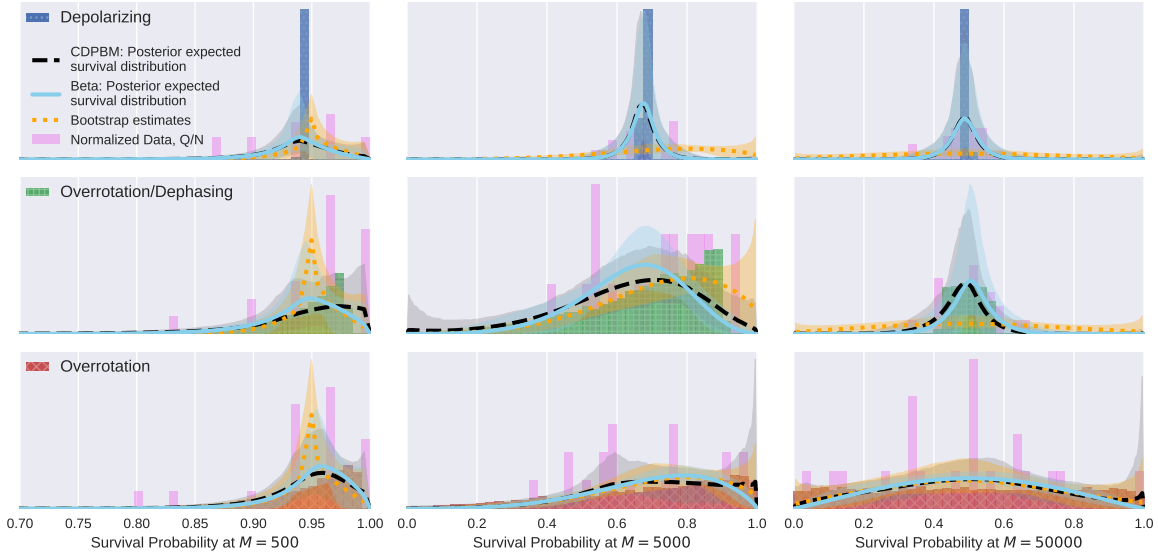


Figure 5: Although the survival distributions at each sequence length are considered to be nuisance parameters of the model, their posteriors are nonetheless interesting and provide a diagnostic check. Here, the three rows correspond to the noise models described in Section 7.1, and each column is a different sequence length. In each plot, Bayes’ estimate of the survival distribution is shown for both models Equation 15 and Equation 13 along with their pointwise 95% credible envelopes. Similar 95% confidence envelopes are shown for the bootstrap method. These are overlaid on top of histograms sampled from the true survival distributions, as well as the (normalized) data that were actually used in the inference.

at a one sided credibility level α ,

$$p_\alpha(D) = [p_0 \text{ such that } \Pr(p > p_0|D) = \alpha]. \quad (26)$$

Here, $\Pr(p|D)$ is the posterior of p under the beta model Equation 13 with the same prior as in Section 7.1 given the RB dataset D . For example, according a given posterior, with 95% probability, $p_{0.95}(D)$ should be a lower bound for the true the value of p . Fixing the model and the prior, the quantity $p_\alpha(D)$ is itself a random variable as it depends on D . What we desire in our numerical test is that consistency condition

$$\Pr(p_\alpha(D) < p_{\text{true}}) \geq \alpha \quad (27)$$

is satisfied for any level α that we care about.

To evaluate this criterion we compute $p_\alpha(D)$ for many simulated datasets D . Each dataset uses the sequence lengths

$$\mathbb{M} = \{1, 100, 200, 500, 1000, 2000, 5000, 10000, 20000, 50000\}$$

and the repetition number $N = 5$. Three-hundred data sets were considered at each of the values $I = 1, 3, 5, 10, 20, 30, 50, 80, 100$. Figure 6 shows both a selection of posteriors, as well as a summary of the distribution of $p_{0.95}(D)$ at each value of I . Note that the sharp elbow displayed in Figure 6(b) could be used in practice to decide on an appropriate amount of data to take: in this example, there is a huge advantage in moving from $I = 5$ to $I = 10$, but not much of an advantage in moving from $I = 10$ to $I = 15$.

The bootstrapped confidence bounds discussed in Section 5.3 are also sensibly defined in the low data regime. In Figure 6(d), however, we see in both parametric and non-parametric bootstrapping that the MLE has a tendency to exaggerate confidence. All bootstrap distributions contain 600 samples.

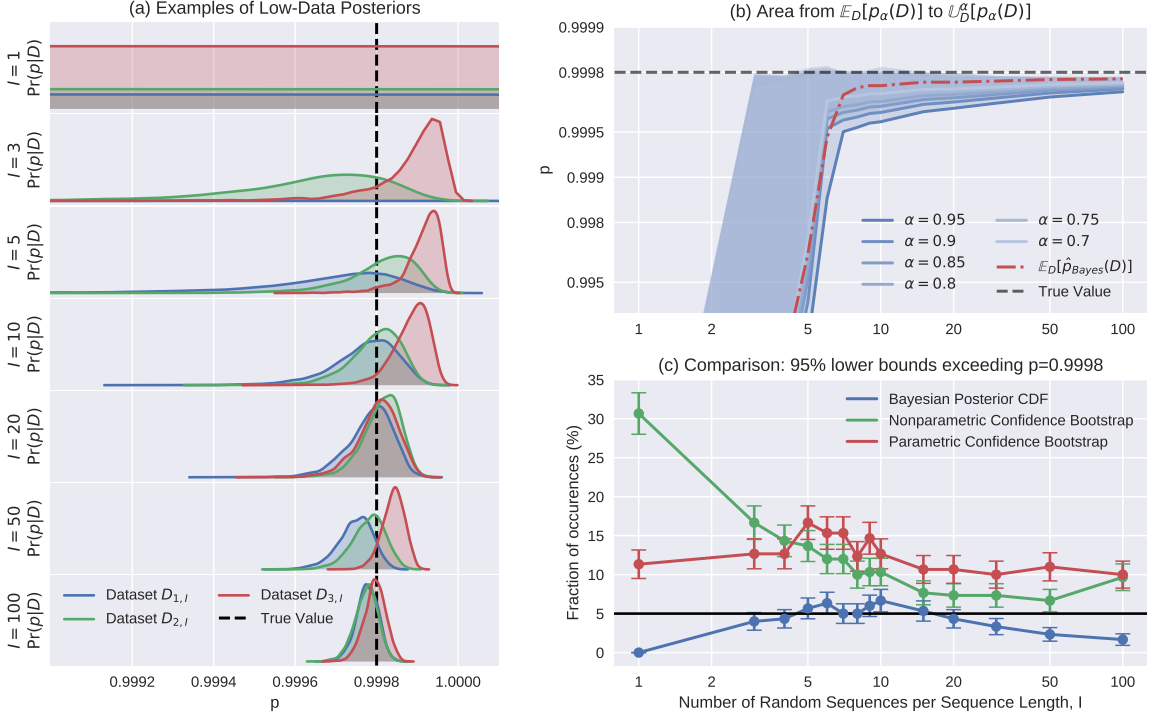


Figure 6: Data from the overrotation model Equation 24c was simulated 300 times for several values of I , the number of random sequences per sequence length. In all cases $|\mathbb{M}| = 10$ sequences were used with $N = 5$ repetitions of each random sequence. Posteriors were computed for every dataset, p -marginals for three of which are shown in (a) for several values of I . (b) The area between the upper $(100 \cdot \alpha)\%$ quantile and the mean value of $p_\alpha(D)$ is shown for several values of α , demonstrating the posterior’s ability to reliably report credible lower bounds for p . (The average value of Bayes’ estimate is shown for comparison.) (c) Finally, we isolate the $\alpha = 0.95$ case and display it along with bootstrapped lower 95% confidence bounds, which do not stay under the desired line. These fractions were computed by running the bootstrap method on the same collections of 300 data sets. Error bars are single standard deviations of simple binomial statistics.

7.3 A pathological model: pushing the Dirichlet process to its limits

To demonstrate that CDPBM based models are capable of handling strange underlying survival distributions, we use a highly pathological error model, constructed to have multiple distinct peaks. The model has gate-independent qubit noise defined as the convex mixture of a channel that resets to a fixed pure state, a channel that resets to identity, and the identity channel, or explicitly

$$\mathcal{E}(\rho) = \text{Tr}(\rho) \left(p_1 |\psi_r\rangle \langle \psi_r| + p_2 \frac{\mathbb{I}}{2} \right) + (1 - p_1 - p_2)\rho. \quad (28a)$$

We used the parameters $p_1 = 0.9$, $p_2 = 0.001$, and $|\psi_r\rangle = e^{-i0.05(X+Y)} |0\rangle$ in our simulations. This noise model results in an average gate fidelity of 0.5495, or a decay base of $p = 0.099$. Due to the high value of p_1 , this error channel is so bad that running RB as a characterization tool is not a great choice in the first place, and therefore looking at the posterior distribution of (p, A, B) is of little

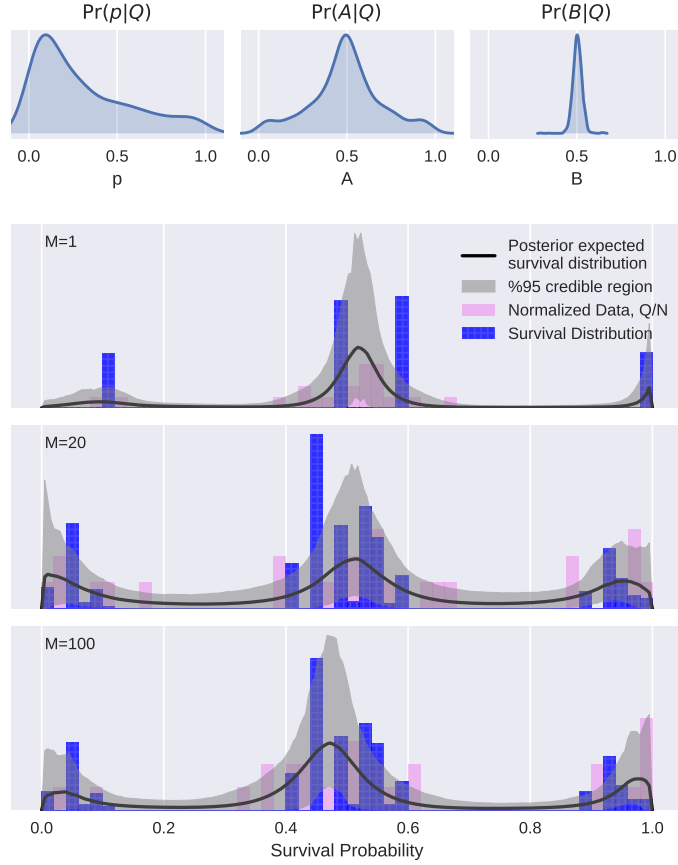


Figure 7: The top row of three plots show marginal posterior distributions of the standard RB protocol tying parameters with data simulated according to the pathological noise model defined in Equation 28. The bottom column of three plots show posterior summaries of the survival distribution at the sequence lengths $M = 1, 20$ and 100 , respectively.

direct use, although similarly bad channels can arise when using interleaved RB to extract tomographic information [32]. In any case, we provide certain marginals at the top of Figure 7 anyway. However, our point is to look at the posterior of the survival parameters, \vec{x}_S , which are summarized in the bottom section of Figure 7. This posterior was computed using the sequence lengths $M = \{1, 2, 5, 20, 50, 100\}$ with $I = 30$ random sequences per sequence length, and $N = 50$ repetitions each. The same gateset as Section 7.1 was used, with the same initial state and measurement operators.

7.4 Complicated Tying Function: Leakage RB (LRB)

There are a few protocols which measure leakage of information into and/or out of the qubit subspace [21, 33, 34, 35]. Here we provide an example using our framework with the LRB protocol that is described in Ref. [21] with an experimental implementation reported as a part of Ref. [36]. We have chosen this protocol because it has one of the most complicated tying functions of existing protocols; for a single qubit there are at least seven tying parameters, three of which are not nuisances. Moreover, it is not quite a SPAM-free protocol—some of the information that is necessary to decouple the three parameters of interest from each other is contained in the constant offset term as well as the coefficients of the exponential terms.

We consider a system with a Hilbert space $\mathcal{X} = \mathcal{X}_1 \oplus \mathcal{X}_2$, where $\dim \mathcal{X}_1 = d_1 = 2$ and $\dim \mathcal{X}_2 =$

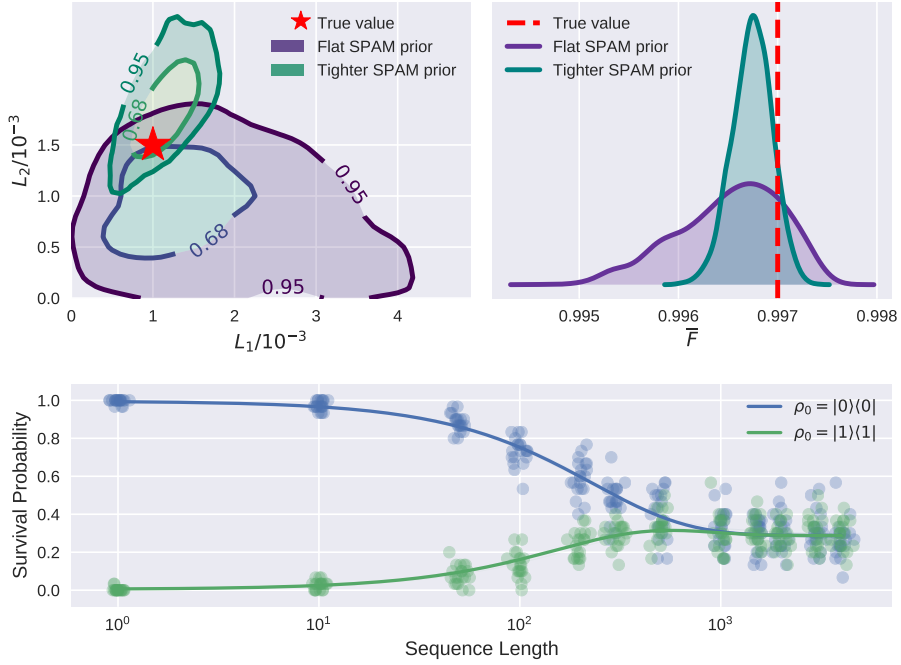


Figure 8: Posterior summaries for the LRB protocol under the model from Equation 13 and two different prior distributions. Simulated data was sampled at $|\mathbb{M}| = 12$ sequence lengths, each with $I = 15$ random sequences and $N = 30$ repetitions per sequence. The joint posterior marginals of the leakage and seepage parameters is shown (top left), as well as the posterior marginals of the average gate fidelity (top right). The LRB tying functions are plotted using parameters randomly drawn from the posterior tying distribution (bottom). Superimposed are the normalized data, where each dot comes from a unique random sequence.

$d_2 = 1$, and \mathcal{X}_1 is the computational subspace. Our noise model is gate independent, equal to the depolarizing leakage extension (DLE) [21] of $\mathcal{E}_{\text{dephasing}} \circ \mathcal{E}_{\text{rot}}$ where

$$\mathcal{E}_{\text{dephasing}}(\rho) = (1 - s)\rho + sZ\rho Z \quad (29a)$$

$$\mathcal{E}_{\text{rot}}(\rho) = e^{-i\alpha Z/2}\rho e^{i\alpha Z/2}, \quad (29b)$$

and where we denote the resulting DLE as \mathcal{E} . The parameters L_1 and L_2 are called the leakage and seepage respectively, and are given by

$$L_1 = 1 - \text{Tr} \mathbb{I}_1 \mathcal{E}(\mathbb{I}_1/d_1) \quad (30a)$$

$$L_2 = \text{Tr} \mathbb{I}_1 \mathcal{E}(\mathbb{I}_2/d_2) \quad (30b)$$

where \mathbb{I}_1 and \mathbb{I}_2 are the projectors onto \mathcal{X}_1 and \mathcal{X}_2 . We see that the leakage quantifies how much population from \mathcal{X}_1 leaks out of \mathcal{X}_1 , and the seepage quantifies how much population seeps into \mathcal{X}_1 from \mathcal{X}_2 . We have assumed that our initial states are prepared in \mathcal{X}_1 for simplicity in this demonstration. We use the values $s = 0.003$, $\alpha = 0.1^\circ$, $L_1 = 0.001$, and $L_2 = 0.0015$. The average gate fidelity of \mathcal{E} averaged over states in \mathcal{X}_1 comes out as $\bar{F} = 0.997001$ with these numbers.

One feature of the fitting method proposed along with the LRB protocol is that it implicitly asserts that certain SPAM parameters sum to unity, and certain other SPAM parameters sum to zero (respectively A and B in our appendix). Though this may be valid for some systems, it depends on the methods of state preparation and measurement for the given device. We have highlighted our ability to loosen this assertion by comparing the posterior distributions due to two priors. In the

first, all SPAM parameters have flat non-informative priors, and in the second, prior information is introduced that causes the two sums in question to have support of roughly $\sim 1(\pm 0.05)$ and $\lesssim 0.05$, respectively. Explicit details of this prior, along with the LRB protocol and how we slightly modified its parameterization can be found in [Section F](#). Posterior results are summarized in [Figure 8](#).

8 Departing from Bernoulli Trials

All models thus far have assumed that measurements conditional on some sequence length and experiment type are Bernoulli trials, or stated differently, we have assumed that two-outcome strong measurements are performed. For some quantum systems, this is not possible, with some other non-binary result being returned from a measurement operation. It would be nice to be able to analyze data from RB and related protocols for these systems too. In this section we point out that our methods extend straight-forwardly (at least in principle) to other measurement schemes.

For example, we can extend the model from [Equation 15](#) to the case of referenced photon counts from a Nitrogen Vacancy center in diamond. In the most commonly used measurement scheme for this system, instead of having direct access to Bernoulli trials with the probability $q = \text{Tr} \tilde{E}_e \tilde{G}_{\vec{j}}(\tilde{\rho}_e)$ for some sequence \vec{j} , we instead have obstructed access to this quantity through the random triplet $(X, Y, Z)|\alpha, \beta$ where $0 < \alpha < \beta$ are unknown Poisson rates [\[37\]](#), giving rise to the likelihood

$$q|G \sim G \tag{31a}$$

$$(X, Y)|\alpha, \beta \sim \text{Pois}(\alpha) \times \text{Pois}(\beta) \tag{31b}$$

$$Z|q, \alpha, \beta \sim \text{Pois}(\beta + (\alpha - \beta)q) \tag{31c}$$

where the prior is exactly the same as in [Equation 13](#) or [Equation 15](#). The subscripts M, e, i were dropped for the sake of brevity.

9 Conclusions and Outlook

We have presented a Bayesian approach to analyzing data from RB+ experiments. We used a formal framework to describe such protocols to emphasize that RB and its derivative protocols, from the perspective of statistical inference, are all quite similar. Specifically, they all admit noise model dependent survival distributions which are tied together parametrically by a combination of quantities of interest and nuisance (SPAM) parameters. A handful of examples are summarized in [Table 1](#).

We proposed a hierarchical Bayesian model that was constructed to be agnostic to the nature of these survival distributions, and hence to the noise model. This was achieved by modeling them non-parametrically through Dirichlet process priors. We also considered modeling them parametrically through the Beta distribution family. For physically reasonable noise models we found that this simpler family worked well. Therefore we suggest using the non-parametric model in, for example, first runs where the system is not well understood, possibly switching to the parametric model when the system is better characterized and RB+ is being used for tune-ups.

Under either model, however, one ends up with a marginal posterior distribution of the RB+ parameters, from which figures of merit can be computed. We found qualitative similarity between the nonparametric MLE bootstrap distribution and the posterior distribution of the Bayesian nonparametric model when using a diffuse prior, which merits further study.

We tested our Bayesian models under various noise types, data regimes, and protocols. Our posterior distributions were computed numerically by drawing posterior samples with MCMC methods. As well as fitting well to survival distributions from standard error models ([Figure 3](#)), we were also able to fit to pathological multi-modal survival distributions ([Figure 7](#)). Due to our choice of parameterization, estimating probabilities very close to the boundaries $[0, 1]$ is stable. Of particular importance, we found no systematic tendency to over-report gate qualities. Specifically, a numerical study of standard

RB in the low data regime showed that posteriors of our model accurately report uncertainty—for example, a 95% credible lower bound on the fidelity is indeed a lower bound to the true value at least 95% of the time (Figure 6). This is in contrast to the frequentist bootstrapping techniques we compared to, which do not always pass this sanity test in the low-data regime.

We assumed throughout this work that the model being used for a given dataset was correct. In practice, features like non-Markovian noise may necessitate corrections to a model. A useful direction of research would therefore be to explore Bayesian model selection and cross validation.

Acknowledgements

IH thanks Robin Blume-Kohout for helpful correspondence regarding frequentist estimators for RB, and Thomas Alexander for numerical MCMC advice.

IH, JJW, and DGC gratefully acknowledge contributions from the Canada First Research Excellence Fund, Industry Canada, Canadian Excellence Research Chairs, the Natural Sciences and Engineering Research Council of Canada, the Canadian Institute for Advanced Research, and the Province of Ontario. CF was supported by the Australian Research Council Grant No. DE170100421. CG was partially supported by the Australian Research Council (ARC) via the Centre of Excellence in Engineered Quantum Systems (EQuS) project number CE110001013 and by the US Army Research Office grant numbers W911NF-14-1-0098 and W911NF-14-1-0103.

References

- [1] J. Emerson, R. Alicki, and K. yczkowski, *Journal of Optics B: Quantum and Semiclassical Optics* **7**, S347 (2005).
- [2] E. Knill, D. Leibfried, R. Reichle, J. Britton, R. B. Blakestad, J. D. Jost, C. Langer, R. Ozeri, S. Seidelin, and D. J. Wineland, *Physical Review A* **77**, 012307 (2008).
- [3] E. Magesan, J. M. Gambetta, and J. Emerson, *Physical Review Letters* **106**, 180504 (2011).
- [4] E. Magesan, J. M. Gambetta, and J. Emerson, *Physical Review A* **85**, 042311 (2012).
- [5] C. Dankert, R. Cleve, J. Emerson, and E. Livine, *Physical Review A* **80**, 012304 (2009).
- [6] K. R. Brown, A. C. Wilson, Y. Colombe, C. Ospelkaus, A. M. Meier, E. Knill, D. Leibfried, and D. J. Wineland, *Physical Review A* **84**, 030303 (2011).
- [7] O. Moussa, M. P. da Silva, C. A. Ryan, and R. Laflamme, *Physical Review Letters* **109**, 070504 (2012).
- [8] M. Veldhorst, J. C. C. Hwang, C. H. Yang, A. W. Leenstra, B. d. Ronde, J. P. Dehollain, J. T. Muhonen, F. E. Hudson, K. M. Itoh, A. Morello, and A. S. Dzurak, *Nature Nanotechnology* **9**, 981 (2014).
- [9] R. Barends, J. Kelly, A. Megrant, A. Veitia, D. Sank, E. Jeffrey, T. C. White, J. Mutus, A. G. Fowler, B. Campbell, Y. Chen, Z. Chen, B. Chiaro, A. Dunsworth, C. Neill, P. OMalley, P. Roushan, A. Vainsencher, J. Wenner, A. N. Korotkov, A. N. Cleland, and J. M. Martinis, *Nature* **508**, 500 (2014).
- [10] J. T. Muhonen, A. Laucht, S. Simmons, J. P. Dehollain, R. Kalra, F. E. Hudson, S. Freer, K. M. Itoh, D. N. Jamieson, J. C. McCallum, A. S. Dzurak, and A. Morello, *Journal of Physics: Condensed Matter* **27**, 154205 (2015).
- [11] T. Xia, M. Lichtman, K. Maller, A. Carr, M. Piotrowicz, L. Isenhower, and M. Saffman, *Physical Review Letters* **114**, 100503 (2015).
- [12] S. Sheldon, L. S. Bishop, E. Magesan, S. Filipp, J. M. Chow, and J. M. Gambetta, *Physical Review A* **93**, 012301 (2016).
- [13] G. Feng, J. J. Wallman, B. Buonacorsi, F. H. Cho, D. K. Park, T. Xin, D. Lu, J. Baugh, and R. Laflamme, *Physical Review Letters* **117**, 260501 (2016).
- [14] R. W. Heeres, P. Reinhold, N. Ofek, L. Frunzio, L. Jiang, M. H. Devoret, and R. J. Schoelkopf, arXiv:1608.02430 [quant-ph] (2016), arXiv:1608.02430 [quant-ph] .

- [15] M. A. Fogarty, M. Veldhorst, R. Harper, C. H. Yang, S. D. Bartlett, S. T. Flammia, and A. S. Dzurak, *Physical Review A* **92**, 022326 (2015).
- [16] J. M. Epstein, A. W. Cross, E. Magesan, and J. M. Gambetta, *Physical Review A* **89**, 062321 (2014).
- [17] H. Ball, T. M. Stace, S. T. Flammia, and M. J. Biercuk, *Physical Review A* **93**, 022303 (2016).
- [18] J. Wallman, C. Granade, R. Harper, and S. T. Flammia, *New Journal of Physics* **17**, 113020 (2015).
- [19] J. Combes, C. Granade, C. Ferrie, and S. T. Flammia, arXiv:1702.03688 [quant-ph] (2017), arXiv:1702.03688 [quant-ph] .
- [20] E. Magesan, J. M. Gambetta, B. R. Johnson, C. A. Ryan, J. M. Chow, S. T. Merkel, M. P. da Silva, G. A. Keefe, M. B. Rothwell, T. A. Ohki, M. B. Ketchen, and M. Steffen, *Physical Review Letters* **109**, 080505 (2012).
- [21] C. J. Wood and J. M. Gambetta, arXiv:1704.03081 [quant-ph] (2017).
- [22] A. Carignan-Dugas, J. J. Wallman, and J. Emerson, *Physical Review A* **92**, 060302 (2015).
- [23] D. Steel, *Synthese* **156**, 53 (2007).
- [24] C. Granade, C. Ferrie, and D. G. Cory, *New Journal of Physics* **17**, 013042 (2015).
- [25] C. A. Ryan, B. R. Johnson, D. Ristè, B. Donovan, and T. A. Ohki, *Review of Scientific Instruments* **88**, 104703 (2017).
- [26] J. B. McDonald and Y. J. Xu, *Journal of Econometrics* **66**, 133 (1995).
- [27] T. J. DiCiccio and B. Efron, *Statistical science* , 189 (1996).
- [28] I. Hincks, J. J. Wallman, C. Ferrie, C. Granade, and D. G. Cory, “Code for ‘bayesian inference for randomized benchmarking protocols’,” (2018).
- [29] S. Duane, A. D. Kennedy, B. J. Pendleton, and D. Roweth, *Physics Letters B* **195**, 216 (1987).
- [30] M. D. Hoffman and A. Gelman, *Journal of Machine Learning Research* **15**, 1593 (2014).
- [31] J. J. Wallman, arXiv:1703.09835 [quant-ph] (2017).
- [32] S. Kimmel, M. P. da Silva, C. A. Ryan, B. R. Johnson, and T. Ohki, *Physical Review X* **4**, 011050 (2014).
- [33] J. J. Wallman, M. Barnhill, and J. Emerson, *Physical Review Letters* **115**, 060501 (2015).
- [34] Z. Chen, J. Kelly, C. Quintana, R. Barends, B. Campbell, Y. Chen, B. Chiaro, A. Dunsworth, A. Fowler, E. Lucero, E. Jeffrey, A. Megrant, J. Mutus, M. Neeley, C. Neill, P. OMalley, P. Roushan, D. Sank, A. Vainsencher, J. Wenner, T. White, A. Korotkov, and J. M. Martinis, *Physical Review Letters* **116**, 020501 (2016).
- [35] T. Chasseur and F. K. Wilhelm, *Physical Review A* **92**, 042333 (2015).
- [36] D. C. McKay, C. J. Wood, S. Sheldon, J. M. Chow, and J. M. Gambetta, arXiv:1612.00858 [quant-ph] (2016).
- [37] I. Hincks, C. Granade, and D. G. Cory, *New Journal of Physics* **20**, 013022 (2018).
- [38] B. Carpenter, A. Gelman, M. Hoffman, D. Lee, B. Goodrich, M. Betancourt, M. Brubaker, J. Guo, P. Li, and A. Riddell, *Journal of Statistical Software, Articles* **76** (2017), 10.18637/jss.v076.i01.
- [39] C. Granade, C. Ferrie, I. Hincks, S. Casagrande, T. Alexander, J. Gross, M. Kononenko, and Y. Sanders, *Quantum* **1**, 5 (2017).
- [40] M. J. Betancourt, arXiv:1304.1920 [stat] (2013).
- [41] Y. W. Teh, in *Encyclopedia of Machine Learning*, edited by C. Sammut and G. I. Webb (Springer US, 2011) pp. 280–287.
- [42] M. D. Escobar and M. West, *Journal of the American Statistical Association* **90**, 577 (1995).
- [43] J. Sethuraman, *Statistica Sinica* **4**, 639 (1994).
- [44] M. Yang, D. B. Dunson, and D. Baird, *Computational Statistics & Data Analysis* **54**, 2172 (2010).
- [45] W. K. Hastings, *Biometrika* **57**, 97 (1970).
- [46] R. M. Neal, arXiv:1206.1901 [physics, stat] (2012).
- [47] M. Betancourt, arXiv:1701.02434 [stat] (2017), arXiv:1701.02434 [stat] .

A Sampling Strategies

For the complete details of our numerical methods there is no better place to look than the code base that accompanies this paper [28]. In this section, we summarize—at a high level—some of the tools and tricks we used.

A.1 Posterior Sampler

Analytic formulae for the posteriors of our models are intractable—we must instead choose a numerical inference algorithm to sample points from the posterior. A sufficient number of these points can be used to compute any quantity of interest related to the posterior. We used the Hybrid Monte Carlo (HMC) sampler using the No-U-Turns (NUTS) heuristic [29, 30]. This is a Markov chain Monte Carlo (MCMC) sampling strategy which has gained widespread use due to its lack of tuning parameters, fast mixing rate, and ability to handle large numbers of parameters. We provide a very brief introduction to MCMC algorithms in Section C. Specifically, we used the PyStan interface to the Stan library [38]. Probabilistic programs such as those written in Equation 13 and Equation 15 can be entered nearly verbatim as input to this library (or other similar libraries), and samples from the posterior are returned. We suspect that sampling algorithms customized to our models could significantly outperform these generic tools, but it is hard to turn down the convenience of modern probabilistic programming languages and automatic differentiation.

It warrants mention why we have not used sequential Monte Carlo (SMC), which has emerged as a popular inference engine for quantum information processing tasks [39], including for RB and IRB with $N = 1$ [24]. Our main reason is that we wish to leave open the option of sampling from exact posterior distributions, especially while still in the proof-of-principle stage. SMC operates by storing the distribution over parameters as a weighted mixture of delta functions. Data is entered sequentially and the prior is gradually transformed into the posterior with the inclusion of each subsequent individual datum. While SMC uses exact likelihood functions to sequentially update the weights with Bayes’ rule, it also occasionally requires a resampling operation that moves the positions of the delta functions to where they are most needed. This resampling step usually only considers the first two moments of the distribution, and tends to distort the distribution toward being multivariate normal—see Appendix B of Reference [39]. Therefore, in SMC, posterior distributions are convolved with normal approximations to the true posterior distribution. However, SMC has an important advantage in that it can naturally be used with adaptive experiments, where the next experiment (sequence length, measurement type, etc.) is chosen based on the current state of knowledge. Also, SMC is often less computationally expensive and always highly parallelizable.

A.2 Reparameterizations

MCMC samplers benefit from using an optimal parameterization of the model — simply reparameterizing a model can make huge differences to the convergence, mixing rates, and stability. Ideally, posterior parameters are decorrelated, centered at the origin, and have a variance of order unity. Doing a perfect job at this would require knowing the posterior in advance of sampling from it, so we must instead rely on other heuristics.

For example, samplers have trouble near hard cutoffs, requiring special boundary specifications, and time can be wasted proposing random-walk values outside of the allowed region. This is relevant to our models where it is common to be inferring values that are physically restricted to the interval $[0, 1]$, and that are ideally very close to the boundary, such as the average gate fidelity of a gate-set. Modern Bayesian inference libraries, such as Stan, will automatically remove hard cutoffs by reparameterizing the model through a logit function for interval constraints, or through the logarithm for one-sided constraints. (It also multiplies the pdf by the change of variables Jacobian so that the prior is not distorted.)

We can do slightly better than this if we have prior expectations about some parameter values. For instance, if we expect a decay parameter p to be on the order of $p_0 = 0.9999$, then instead of using the sampling variable $\tilde{p} = \text{logit}(p)$ as would automatically be done by Stan, we can use the variable p_{err} where $p = \text{logit}(p_0 + p_{\text{err}})$. This is distinct from the role of a prior distribution in the sense that the correct distribution is sampled from even if we have set p_0 far from the value p that we are attempting to estimate; rather, we arrive at our samples less efficiently in that case. For reference, $\text{logit}(0.9999) \approx 9$, and we will have, with very little effort, prevented the sampler from making an initial random walk from 0 to 9 while also keeping track of 200 other variables.

If we additionally have expectations about the standard deviation, say we expect $\delta p = p_0 \pm \delta p$ in the posterior, then we can use the changed variable p_{err} where $p = \text{logit}(p_0 + \delta \tilde{p} \cdot p_{\text{err}})$. If we let $\delta \tilde{p} = \delta p \cdot p_0^{-1}(1 - p_0)^{-1}$, then $p_{\text{err}} = 0 \pm 1$ will translate to $p = p_0 \pm \delta p$. This trick does not affect the posterior in any way, it only improves sampling performance. We have had success using least-squared fits to estimate p_0 and/or δp (along with other parameters), using these values in the parameter transformation. If there is not enough data to meaningfully estimate δp with, for example, a weighted least squares fit, then $\delta \tilde{p} = 0.5$ is a fine choice.

The above heuristic should apply well to most probability parameters. There is a notable exception that comes up in low data regimes, which we will now illustrate in the case of standard RB for concreteness. Here, the tying function is $(A - B)p^M + B$, and for high quality devices, and at very low values of M , the survival probability is roughly equal to $A \lesssim 1$. Moreover, low values of M are exactly where we learn the most about A , allowing us to decorrelate its value from p and B . Suppose, however, that we are in the low data regime defined by $1/(1 - A) \gg N \cdot I$, so that at the lowest values of M it's very likely that every single shot of the experiment will return 1. In this case any estimation technique will only be capable of producing a lower bound on the value of A ; any value of A arbitrarily close to 1 will be consistent with the data. This is a problem for the logit rescaling discussed above because an estimate of A arbitrarily close to 1 implies a sampling parameter A_{err} that is arbitrarily large no matter the choices of A_0 and δA . There are a few potential paths forward. One is to switch sampling strategies to something like Riemannian Manifold HMC that fairs better with varying curvature in parameter space [40]. Another is to reparameterize in a different way, for example through an exponential distribution. Perhaps the easiest, however, is to recall that the lowest values of M are dubious in the case of gate dependent noise, and no data should be taken there anyway. We can just take a new definition of the initial state to be our old initial state acted on by a fixed number of random gates, effectively lowering the value of A .

B Nonparametric Families

B.1 Dirichlet Processes

Dirichlet processes (DP) can be introduced in many ways. Given how they are used in the main body of this paper, we will introduce them as a natural extension to beta and Dirichlet priors as follows. Much more comprehensive introductions can be found elsewhere, for example, see this article of Teh [41].

First, consider of coin with an unknown bias p that we wish to infer. If we flip it N times and sum the resulting number of heads we get the random variable $X \sim \text{Binom}(N, p)$. In a Bayesian setting, we start by assigning a prior $\pi(p)$ to the unknown quantity p . Having collected the variate x of X , our posterior is proportional to $\Pr(p|x) \propto \int \binom{N}{x} p^x (1 - p)^{N-x} d\pi_p(p)$. An important property the beta distribution is that when it is used as the prior in this example, say $\pi(p) = \text{Beta}(a, b)$ for some choices $a > 0$ and $b > 0$, then this integral has a nice closed form solution,

$$\Pr(p|x) = \text{Beta}(a + x, b + N - x). \tag{32}$$

This is one of the reasons the beta distribution family is the canonical family of distributions with support on $[0, 1]$. Moreover, from this formula, an operational interpretation of the prior parameters a and b is apparent: a can be thought of as the number of prior ‘heads’ observations, and b as the number

of prior ‘tails’ observations. For example, $\pi(p) = \text{Beta}(1, 1)$ is asserting that one’s prior knowledge of p is equivalent to having already flipped the coin twice, with each a heads and a tails landing once.

Let us generalize one step further before mentioning Dirichlet processes. Suppose we are interested in inferring the weights $p = (p_1, \dots, p_K)$ of a K -sided die, where p is a finite probability distribution, so that $\sum_k p_k = 1$ and $p_k \geq 0$. (The coin example above is the case $K = 2$.) Rolling this die N times and binning the number of times each side lands face up results in the random variable $X = (X_1, \dots, X_K) \sim \text{Multinomial}(N, p)$. The Dirichlet distribution family is the natural extension to the beta distribution family for $K > 2$. Namely, if we set the prior $\pi(p) = \text{Dir}(a_1, \dots, a_K)$, then the posterior distribution is given by

$$\Pr(p|x) = \text{Dir}(a_1 + x_1, \dots, a_K + x_K) \quad (33)$$

where $x = (x_1, \dots, x_K)$ is the data. As before, this provides an operational interpretation of the prior parameters a_1, \dots, a_K — the value a_k can be interpreted as the number of prior observations of side k out a total of $\sum_k a_k$ prior observations.

Dirichlet processes can be thought of as the next logical step in this progression. We move from probability distributions with two sides, to K sides, and now to a continuum of sides; Dirichlet processes are natural priors for probability density functions. Suppose that f is an unknown probability density function on the sample space Ω that we wish to infer. Therefore $\int_{\Omega} f(x) d\mu(x) = 1$ where μ is some measure on Ω . Data is collected from this unknown distribution through the random variable $X \sim f$. We wish to set our prior on f to be a Dirichlet process, which is a distribution of distributions on the sample space Ω . First, we need to define what a Dirichlet process is: given a distribution G_0 defined on Ω and a positive real number $\alpha > 0$, we say that the random distribution G is Dirichlet process distributed with base distribution G_0 and concentration parameter α , writing $G \sim \text{DP}(\alpha, G_0)$ to denote this, if for any finite disjoint measurable partition $\cup_{k=1}^K B_k = \Omega$, it holds that

$$(G(B_1), \dots, G(B_K)) \sim \text{Dir}(\alpha G_0(B_1), \dots, \alpha G_0(B_K)). \quad (34)$$

Note that for $B \subset \Omega$, all we mean by $G(B)$ is the probability of an event in B under distribution G . This means that $\alpha G_0(B)$ has the interpretation of being the number of prior observations in the region $B \subset \Omega$, and that to be Dirichlet process distributed means to be a distribution which obeys this condition for every possible partition of Ω into regions. In our previous example with the K -sided die, we could have reparameterized the Dirichlet prior as $\text{Dir}(\alpha, g)$ where $\alpha := \sum_k \alpha_k$ and $g := (\alpha_1/\alpha, \dots, \alpha_K/\alpha)$ to be more notationally analogous to the present example.

If we let $\pi(f) = \text{DP}(\alpha, G_0)$ be the prior distribution of f , and suppose we make N iid measurements $X \sim f$, then the posterior is also Dirichlet process distributed, with

$$\Pr(f|x) = \text{DP} \left(\alpha + N, \frac{\alpha}{\alpha + N} G_0 + \frac{N}{\alpha + N} \frac{\sum_{k=1}^N \delta_{x_k}}{N} \right) \quad (35)$$

where δ_{x_k} is the delta distribution centered at the datum $x_k \in \Omega$. We see that the base distribution of the posterior of f is a mixture of the prior’s base distribution and the empirical distribution of the data. It also makes it clear that α still has the interpretation as the total number of prior observations. Despite these nice interpretations, so far it might seem like Dirichlet processes are too abstractly defined to make them practical; at the end of this section, we will see that they have a alternate and procedural description which is not too hard to work with.

Dirichlet processes can be used as a generic stand-in for parametric priors in Bayesian models. For example, suppose we have samples $X_k | \lambda \sim \text{Pois}(T_k \lambda)$ for some rate of events λ measured for durations of time T_k . Moreover, suppose that there is not just one underlying rate of emission, but that there truly is a distribution of rates taking place, and we would like to infer what this distribution looks like. A parametric Bayesian approach might be through the model

$$\begin{aligned} X_k | \lambda &\sim \text{Pois}(T_k \lambda) \\ \lambda &\sim \text{Gam}(a, b) \\ a, b &\sim \pi(a, b) \end{aligned} \quad (36)$$

where $\pi(a, b)$ is some prior on a and b . We have parameterized the unknown distribution over rates with a gamma distribution with hyperparameters a and b ; if we infer a and b , we can plot an estimate of the distribution of λ . However, if we are unable to confidently assert that the distribution over rates λ must be gamma distributed, then we might choose a *nonparametric* Bayesian approach with the model

$$\begin{aligned} X_k | \lambda &\sim \text{Pois}(T_k \lambda) \\ \lambda &\sim G \\ G &\sim \text{DP}(\alpha, G_0). \end{aligned} \tag{37}$$

Just as we looked at the posterior of the parameters a and b above, here we can look at the posterior of G .

One caveat to random distributions drawn from $\text{DP}(\alpha, G_0)$ is that they are almost surely discrete in nature, even when G_0 is a continuous distribution. With probability one, $G \sim \text{DP}(\alpha, G_0)$ will be of the form

$$G(\cdot) = \sum_{k=1}^{\infty} p_k \delta_{\theta_k}(\cdot) \tag{38}$$

where the p_k are probabilities summing to unity and θ_k are members of Ω . However, this is not a big deal in practice for two reasons. The first is that any continuous function can be approximated with arbitrary accuracy in L_1 distance using distributions of the form [Equation 38](#). Secondly, we always have the option of convolving G with some smooth distribution to end up with a smooth distribution. This is called a Dirichlet process *mixture model* [\[42\]](#).

Sethuraman found a way to construct instances of $\text{DP}(\alpha, G_0)$ in the form of [Equation 38](#) using a *stick breaking process* [\[43\]](#). A random variate $G \sim \text{DP}(\alpha, G_0)$ can be constructed as follows. The points θ_k are simply drawn from G_0 independently and identically. Their weights p_k , however, are derived from the following process. A stick of unit length is broken in two at the random location $V_1 \sim \text{Beta}(1, \alpha)$. The first piece is kept and its length is assigned to the first weight, $p_1 = V_1$. The remaining piece has length $1 - V_1$ and is broken again at a random fraction $V_2 \sim \text{Beta}(1, \alpha)$ of its length. The first piece is kept and its length is assigned to the second weight, $p_2 = V_2(1 - V_1)$. This process is repeated until the stick has been broken up a countably infinite number of times, giving $p_k = V_k \prod_{l < k} (1 - V_l)$. We therefore have the representation

$$\begin{aligned} G &= \sum_{k=1}^{\infty} \left[V_k \prod_{l=1}^{k-1} (1 - V_l) \right] \delta_{\theta_k} \\ V_k &\stackrel{\text{iid}}{\sim} \text{Beta}(1, \alpha), \quad \theta_k \stackrel{\text{iid}}{\sim} G_0 \end{aligned} \tag{39}$$

which is equivalent to $G \sim \text{DP}(\alpha, G_0)$.

Finally, we remark that it is standard practice to assign a distribution to the parameter α , acknowledging one doesn't know *a priori* how good the base distribution G_0 is. We can see this in the stick breaking process, where low values of α lead to few important modes, and high values of α lead to many modes. In practice, Dirichlet processes are parameterized by their weights and locations, and the number of possible modes is truncated. One can verify that a certain truncation is sufficient by making sure the last weights (which must decrease in size) are negligibly small.

B.2 Constrained Dirichlet Process Beta Mixtures

We wish to modify the Dirichlet Process, defined in the previous section, so as to make it a suitable prior for survival distributions. In order for such a prior to work well with state-of-the-art MCMC samplers, which depend on gradients, we require a sample space of smooth distributions. This is

easily done, as in the previous section, by convolving variates of the Dirichlet process with smooth distributions. It is natural for us to convolve with Beta distributions rather than the typically used normal distributions because survival distributions have support only within the interval $[0, 1]$.

The main difficulty of our construction lies in our second demand, which is the ability to constrain certain moments of these random distributions to specific values. We draw inspiration from Yang et al. [44] who propose a method to specify either or both of the first two moments of Dirichlet process variates. This method consists simply of shifting and scaling the delta locations θ_k (see Equation 39) so that the mean and variance of G are as desired. We cannot use this approach directly because our domain is $[0, 1]$; for example, we might need to shift some of our locations θ_k to be outside of this interval to obtain the correct mean, which is not allowed. To overcome this, we use the logit function and its inverse to constrain and unconstrain variables between \mathbb{R} and $(0, 1)$, as follows.

Using a sample space $\Omega = \mathbb{R} \times (0, 1)$, we begin by drawing a standard Dirichlet process distributed variate $\sum_{k=1}^K w_k \delta_{(\nu_k^*, r_k)}$. Here, r_k is the scaled variance parameter (Section D) and ν_k^* represents an unconstrained beta mean. We then constrain each of these latter values to $(0, 1)$ by using the inverse logit function, $\nu_k = \text{logit}^{-1}(\nu_k^* + h) = 1/(1 + e^{-\nu_k^* - h})$. The value of h is chosen as the unique real number which enforces the condition $\sum_{k=1}^K w_k \nu_k = \mu_1$. This in turn guarantees that $\mathbb{E}[G] = \mu_1$. There is no analytic formula for h , but it can be found efficiently with numerical optimization. In particular, Newton's method with an initial guess $h = \text{logit}(\mu_1 - \sum_{k=1}^K w_k \nu_k^*)$ has quadratic convergence. A code sample is shown in Listing 1. This procedure produces a variate from what we call the mean-constrained Dirichlet process beta mixture mean-CDPBM distribution, which is summarized in Equation 14 of the main body.

Draws from the second-moment-constrained version, $\text{CDPBM}_K(\alpha, G_0, \mu_2)$, and the first-second-moment-constrained version, $\text{CDPBM}_K(\alpha, G_0, (\mu_1, \mu_2))$, are similar, except that a transform of the form $\text{logit}^{-1}(h_1 \nu^* + h_2)$ is necessary to constrain the variance as well as the mean.

If a protocol were to tie together the first two moments, following Equation 15, we would have the probabilistic program

$$\vec{x}_T \sim \pi(\vec{x}_T) \tag{40a}$$

$$\mu_{1,M,e} | \vec{x}_T = T(1, M, e, \vec{x}_T) \tag{40b}$$

$$\mu_{2,M,e} | \vec{x}_T = T(2, M, e, \vec{x}_T) \tag{40c}$$

$$\alpha_{M,e} \stackrel{\text{iid}}{\sim} \text{Gam}(1, 1) \tag{40d}$$

$$G_{M,e} | \alpha_{M,e}, \mu_{1,M,e}, \mu_{2,M,e} \stackrel{\text{ind}}{\sim} \text{CDPBM}_K(\alpha_{M,e}, G_0, (\mu_{1,M,e}, \mu_{2,M,e})) \tag{40e}$$

$$q_{M,e,i} | G_{M,e} \stackrel{\text{ind}}{\sim} G_{M,e} \tag{40f}$$

$$Q_{M,e,i} | q_{M,e,i} \stackrel{\text{ind}}{\sim} \text{Binom}(N, q_{M,e,i}). \tag{40g}$$

Listing 1: Stan function (similar to C) to transform input weighted locations (ν_k^*) into output locations (ν_k) whose weighted mean is equal to μ .

```

// nu_star is a vector of input locations
// w is a length-K vector of weights
// mu is the desired mean value
vector compute_nu(vector nu_star, vector w, real mu) {

    real h;
    vector [size[w]] nu;

```

```

// initial guess for h is exact when var(nu_star)=0
h = logit(mu) - dot_product(w, nu_star);

// fixed descent of five steps
for (newton_loops in 1:5) {
    nu = inv_logit(h + nu_star);
    h = h - (dot_product(w, nu) - mu) /
           (dot_product(w, nu .* (1-nu)));
}

nu = inv_logit(h + nu_star);

return nu;
}

```

C MCMC Introduction

A Markov chain Monte Carlo (MCMC) method is an algorithm used to sample independent elements from some desired distribution using the following general principle: an instance of a Markov chain is simulated, where the Markov chain has been designed to have a steady-state distribution equal to the distribution of interest.

The Metropolis–Hastings is one of the simplest such algorithms. It is designed for the scenario where one wants to sample from the density function $f(x)$ but one only has access to an unnormalized version $g(x)$, where $f(x) = g(x) / \int g(x)dx$ [45]. This is often useful in the context of Bayesian inference where $f(x) = \Pr(x|d)$ is the posterior of x given the data d . By Bayes’ law, $f(x) \propto \Pr(d|x)\pi(x)$ where both the likelihood $\Pr(d|x)$ and prior $\pi(x)$ are known, but the normalization constant $\int \Pr(d|x)\pi(x)dx$ is intractable.

The Metropolis–Hastings trick is to construct a Markov chain whose steady state distribution is given by $f(x)$, but for which simulating a random instance requires only evaluations of ratios of f , which are the same as ratios of g . Then we may start with an arbitrary initial value and evolve until we have reason to believe we are in the steady state, which is determined either empirically or theoretically. The last time sample represents a random sample drawn from $f(x)$. If multiple samples are required, it is common to, say, throw out the first 1000 transient time points of the process (the *burn-in* period), and keep every 100th subsequent time step as a random sample of $f(x)$. A short auto-correlation time post burn-in, known as a fast *mixing rate*, is desired, so that fewer samples need to be thrown out.

The algorithm requires a *proposal density* $h(x'|x)$ whose job is to propose the next value of the process, x' , given the previous value, x . The prototypical choice is a normal distribution $h(x'|x) \propto e^{-(x-x')^2/2\sigma^2}$. This choice affects the burn-in time and mixing rate. For example, with a normal proposal density, a small variance will mean it takes many steps to move around the domain of f leading to a slow mixing rate. On the other hand, a large variance may usually propose new locations well outside the likely support of f , leading to high rejection rates and therefore also slow mixing. A well-tuned proposal density will hit the sweet spot.

The algorithm is as follows:

1. Somehow pick an initial value, x_0 .
2. For $k \geq 1$, draw a proposal and a random number,

$$\begin{aligned}
 x' &\sim h(x'|x_{k-1}) \\
 r &\sim \text{Unif}([0, 1]),
 \end{aligned}$$

and then set $x_k = \begin{cases} x' & \text{if } r \leq g(x')/g(x_{k-1}) \\ x_{k-1} & \text{else} \end{cases}$.

3. Iterate the previous step until the desired number of samples from the steady-state have been acquired.

Intuitively this makes sense; we move from the previous location x_{k-1} to the proposed location x' with a probability that prefers a higher density of f , characterized by $f(x')/f(x_{k-1}) = g(x')/g(x_{k-1})$. Therefore samples will end up in the densest regions of $f(x)$.

The simulation method used in our paper is Hamiltonian Monte carlo (HMC) which is just a more sophisticated MCMC method [46]. Here, the term Hamiltonian is used in the classical context. The unknown distribution $f(x)$ is treated as being the Boltzmann distribution of some energy function over states in the sample space. The proposal for the next step in the Markov chain simulation is drawn by simulating the dynamics of this Hamiltonian system using the previous sample as the starting point and a random initial momentum for some amount of time — the endpoint of the trajectory is the proposal. This results in very large steps and greatly decreases the mixing time; a well tuned HMC sampler has nearly no correlation between adjacent points. The main improvement made by the No-U-Turns sampler was to introduce an automatic way to determine how long to simulate each Hamiltonian trajectory for [30]. A recent conceptual tutorial on Hamiltonian Monte Carlo has been provided by Betancourt [47].

D Beta Reparameterizations

In this section we provide some useful reparameterizations of the beta distribution, along with their inverses. As noted in Equation 11 of the main body, a beta distribution $\text{Beta}(\alpha, \beta)$ has a density function given by

$$\text{pdf}_{\text{Beta}}(q) = \frac{q^{\alpha-1}(1-q)^{\beta-1}}{\text{B}(\alpha, \beta)} \quad (41)$$

for any $q \in [0, 1]$. The normalization constant $\text{B}(\alpha, \beta)$ is the beta function, which is defined in terms of the gamma function, $\text{B}(\alpha, \beta) = \frac{\Gamma(\alpha)\Gamma(\beta)}{\Gamma(\alpha+\beta)}$. The parameters α and β must both be positive. Its mean and variance are given by

$$\mu = \frac{\alpha}{\alpha + \beta} \quad (42a)$$

$$\sigma^2 = \frac{\alpha\beta}{(\alpha + \beta)^2(\alpha + \beta + 1)} \quad (42b)$$

respectively. The conditions $\alpha, \beta > 0$ are exactly equivalent to the conditions $0 < \mu < 1$ and $0 < \sigma^2 < \mu(1 - \mu)$.

The parameters α and β have operational interpretations in terms of ‘prior observations’; α is the number of prior observations of heads, and β is the number of prior observations of tails. Therefore, for example, the uniform prior $\text{Beta}(1, 1)$ asserts that two prior observations have been made: one of heads, and one of tails. not entirely intuitive. In Table 2, four reparameterizations along with their inverse transformations are given.

E Priors on Heavily Biased Coins

In all of the examples in the main text we used an uninformative uniform prior on probability parameters such as A , B , and p in the standard RB protocol. There may be situations, especially in low data regimes, where incorporating prior knowledge has a noticeable effect on the posterior width, thereby reducing the necessary amount of data needed to attain a desired credibility lower bound.

Parameters	Bounds	Transform	Inverse Transform	Variance
(μ, σ^2)	$\mu \in (0, 1)$ $\sigma^2 \in (0, \mu(1 - \mu))$	$\mu = \alpha/(\alpha + \beta)$ $\sigma^2 = \alpha\beta/((\alpha + \beta)^2(\alpha + \beta + 1))$	$\alpha = \mu^2(1 - \mu)/\sigma^2 - \mu$ $\beta = \mu(1 - \mu)^2/\sigma^2 - (1 - \mu)$	σ^2
(μ, μ_2)	$\mu \in (0, 1)$ $\mu_2 \in (\mu^2, \mu)$	$\mu = \alpha/(\alpha + \beta)$ $\mu_2 = \alpha(1 + \alpha)/(\alpha + \beta)(1 + \alpha + \beta)$	$\alpha = \mu(\mu - \mu_2)/(\mu_2 - \mu^2)$ $\beta = (1 - \mu)(\mu - \mu_2)/(\mu_2 - \mu^2)$	$\sigma^2 = \mu_2 - \mu^2$
(μ, t)	$\mu \in (0, 1)$ $t \in (0, 1)$	$\mu = \alpha/(\alpha + \beta)$ $t = 1/(1 + \alpha + \beta)$	$\alpha = \mu(1/t - 1)$ $\beta = (1 - \mu)(1 - t)/t$	$\sigma^2 = t\mu(1 - \mu)$
(μ, r)	$\mu \in (0, 1)$ $r \in (0, 1)$	$\mu = \alpha/(\alpha + \beta)$ $r = (\alpha + \beta)^2/(\alpha\beta(1 + \alpha + \beta))$	$\alpha = 1/(r - r\mu) - \mu$ $\beta = 1/(r\mu) + \mu - 1$	$\sigma^2 = r\mu^2(1 - \mu)^2$
(μ, s)	$\mu \in (0, 1)$ $s \in (0, \infty)$	$\mu = \alpha/(\alpha + \beta)$ $s = \alpha + \beta$	$\alpha = s\mu$ $\beta = s(1 - \mu)$	$\sigma^2 = \mu(1 - \mu)/(s + 1)$

Table 2: Five reparameterizations of the beta distribution $\text{Beta}(\alpha, \beta)$. The first two, (μ, σ^2) and (μ, μ_2) , simply reparameterizes into mean and variance (or second moment), which yields non-rectangular bounds. The other three parameterizations have rectangular bounds. In the parameterization (μ, t) , t represents the fraction of the maximum possible variance given a mean μ . Conversely, in the parameterization (μ, s) , we have $t = 1/(s + 1)$ so that large s corresponds to small variance. The parameterization (μ, r) is the only one that does not allow the full range of variance – the maximum possible variance (assuming $0 < r < 1$) is $\mu^2(1 - \mu)^2$. This prevents build-up of mass at the boundaries 0 and 1 by forcing both the constraints $\alpha > 1$ and $\beta > 1$.

For this purpose, we suggest a two-parameter family of distribution with support on $[0, 1]$ which we call *probably at least* (PAL). A member of this family with parameters $0 < p_0 < 1$ and $0 < z < p_0$ has a continuous density function given by

$$\text{pdf}_{\text{PAL}}(x) = \frac{1 - z}{1 - p_0} \begin{cases} \left(\frac{x}{p_0}\right)^{\frac{p_0 - z}{z(1 - p_0)}} & x < p_0 \\ 1 & x \geq p_0 \end{cases}. \quad (43)$$

This distribution is a sort of hedged version of $\text{Unif}([p_0, 1])$ that admits a finite but decreasing probability that $x < p_0$. Indeed, it is parameterized so that the probability $0 < x < p_0$ is equal to z . Observe that $p_0 = z$ gives $\text{Unif}([0, 1])$, and $z \rightarrow 0$ approaches $\text{Unif}([p_0, 1])$.

If the discontinuity of the derivative of this prior at $x = p_0$ poses a problem for the sampler at hand, this distribution can be smoothed over as follows:

$$g(x) = \frac{p_0^2(2 - z) + 2xz + p_0(2x + z)}{zp_0(1 - p_0)}$$

$$\text{pdf}_{\text{PAL}'}(x) = \frac{1 - z}{1 - p_0} \begin{cases} g(x) \left(\frac{x}{p_0}\right)^{2\frac{p_0 - z}{z(1 - p_0)}} & x < p_0 \\ 1 & x \geq p_0 \end{cases}. \quad (44)$$

The parameters p_0 and z have the same interpretations, but now the decaying piece moves smoothly into the constant piece, at the cost of a bit more complexity.

F A Reparameterization of LRB

Consider SPAM configurations $e = (\lambda, i) \in \mathfrak{E}$ where E_λ is a measurement operator, and ρ_i is an initial state. LRB as described in [21] has a first moment tying function $T(1, M, e, \vec{x}_T)$ defined by

$$\begin{aligned} & \frac{1}{L_1 + L_2} \text{Tr} \left[E_\lambda^\dagger \mathcal{E} \left(L_2 \frac{\mathbb{I}_1}{d_1} + L_1 \frac{\mathbb{I}_2}{d_2} \right) \right] \\ & + \left(\frac{L_1}{L_1 + L_2} - p_i \right) \text{Tr} \left[E_\lambda^\dagger \mathcal{E} \left(\frac{\mathbb{I}_1}{d_1} - \frac{\mathbb{I}_2}{d_2} \right) \right] \lambda_1^M \\ & + (1 - p_i) \text{Tr} \left[E_\lambda^\dagger \mathcal{E} \left(\rho'_i - \frac{\mathbb{I}_1}{d_1} \right) \right] \lambda_2^M \end{aligned} \quad (45)$$

where \mathcal{E} is the gate independent noise acting on $\mathcal{X}_1 \oplus \mathcal{X}_2$, with $\dim \mathcal{X}_k = d_k$ and $\mathbb{I}_k = \mathbb{I}_{\mathcal{X}_k}$ for $k = 1, 2$. Here, $p_i := \text{Tr}[\mathbb{I}_1 \rho_i]$ and $\rho'_i := \mathbb{I}_1 \rho_i \mathbb{I}_1 / (1 - p_i)$. The protocol recommends choosing $\lambda = 0, \dots, d_1 - 1$ with $E_\lambda \approx |\lambda\rangle \langle \lambda|$ and $i = 0$ with $\rho_0 \approx |0\rangle \langle 0|$. Other quantities are defined as

$$L_1 = 1 - \text{Tr} \mathcal{E}(\mathbb{I}_1/d_1) \mathbb{I}_1 \quad (46a)$$

$$L_2 = \text{Tr} \mathcal{E}(\mathbb{I}_2/d_2) \mathbb{I}_1 \quad (46b)$$

$$\lambda_1 = 1 - L_1 - L_2 \quad (46c)$$

$$\lambda_2 = \mu_1(1 - L_1) = \frac{d_1 \overline{F}(\mathcal{E}) - (1 - L_1)}{d_1 - 1} \quad (46d)$$

with $\overline{F}(\mathcal{E})$ the average gate fidelity of \mathcal{E} averaged over states in \mathcal{X}_1 . L_1 , called the *leakage*, measures \mathcal{E} 's average loss of population from \mathcal{X}_1 into \mathcal{X}_2 , and L_2 , called the *seepage*, measures the reverse effect. Some easy bounds on these parameters include

$$L_1, L_2 \geq 0 \quad (47a)$$

$$L_1 + L_2 \leq 1. \quad (47b)$$

Wood and Gambetta suggest extracting the parameters of interest, (L_1, L_2, \overline{F}) , as follows. First, the data are summed over λ and the sample mean is taken over sequences I and sequence repetitions N . Under this sum the third term of the tying function, $\sum_\lambda \text{Tr} \left[E_\lambda^\dagger \mathcal{E} \left(\rho'_0 - \frac{\mathbb{I}_1}{d_1} \right) \right] \approx 0$, approximately cancels out leaving a single exponential term of base λ_1 . Fitting to this curve yields λ_1 and hence $L_1 + L_2$, and combining this with the constant offset of the curve, $\sum_\lambda \frac{1}{L_1 + L_2} \text{Tr} \left[E_\lambda^\dagger \mathcal{E} \left(L_2 \frac{\mathbb{I}_1}{d_1} + L_1 \frac{\mathbb{I}_2}{d_2} \right) \right] \approx \frac{L_2}{L_1 + L_2}$, we can separate to get L_1 and L_2 . Note that this protocol is not truly SPAM free because part of the inference relies on the constant term which contains SPAM parameters. Next we go back to the unsummed data, plug in our estimate of λ_1 , and fit to λ_2 to deduce \overline{F} .

In our scheme, we are able to process the data all at once, instead of this two step fitting procedure. It is helpful to rewrite the tying function a bit to make it a bit more clear what all of the independent parameters are. We generalize the protocol to possibly use multiple initial states ρ_i , $i = 0, \dots, d - 1$. Then if we define $A_\lambda = \text{Tr}[E_\lambda^\dagger \mathcal{E}(\mathbb{I}_1/d_1)]$, $B_\lambda = \text{Tr}[E_\lambda^\dagger \mathcal{E}(\mathbb{I}_2/d_2)]$, and $C_{i,\lambda} = \text{Tr}[E_\lambda^\dagger \mathcal{E}(\rho_i)]$ the tying function is expressed as

$$\begin{aligned} T(1, M, (\lambda, i), \vec{x}_T) &= \frac{L_2 A_\lambda + L_1 B_\lambda}{L_1 + L_2} \\ &+ \left(\frac{L_1}{L_1 + L_2} - p_i \right) (A_\lambda - B_\lambda) \lambda_1^M \\ &+ (1 - p_i) (C_{i,\lambda} - A_\lambda) \lambda_2^M. \end{aligned} \quad (48)$$

There are two reasons that one might prefer to use an orthogonal basis of pure initial states with one measurement operator, rather than vice versa, as suggested in the LRB paper. The first is that it

requires fewer nuisance parameters — both A_λ and B_λ depend on the measurement but not the initial state. The second is that the offset term $\frac{L_2 A_\lambda + L_1 B_\lambda}{L_1 + L_2}$ is exactly equal for all experiments (under the assumption of gate-independent noise), which means it can effectively be measured independently by including very long sequence lengths in the data collection.

In [Section 7.4](#) of the main text, we used one measurement operator, $M = 0.99999 |0\rangle\langle 0|$, and two initial states, $\rho_0 = 0.9999 |0\rangle\langle 0|$ and $\rho_1 = 0.9995 |1\rangle\langle 1|$. The two prior distributions used for tying parameters were

$$L_1, L_2, \cdot \sim \text{Dir}(1, 1, 100) \tag{49a}$$

$$\mu_1, A_\lambda, B_\lambda, C_{i,\lambda} \sim \text{Unif}([0, 1]). \tag{49b}$$

and

$$L_1, L_2, \cdot \sim \text{Dir}(1, 1, 100) \tag{50a}$$

$$\mu_1, C_{i,\lambda} \sim \text{Unif}([0, 1]) \tag{50b}$$

$$A_\lambda \sim \text{Beta}(100, 100) \tag{50c}$$

$$B_\lambda \sim \text{Beta}(1, 100) \tag{50d}$$

labeled ‘Flat SPAM prior’ and ‘Tighter SPAM prior’ in [Figure 8](#), respectively. The Dirichlet distribution on L_1 and L_2 was chosen because of the additive constraint $L_1 + L_2 \leq 1$ means that the triple $(L_1, L_2, 1 - L_1 - L_2)$ is a probability vector. The variable $0 \leq \mu_1 \leq 1$ has the interpretation of the depolarizing parameter of \mathcal{E} restricted to \mathcal{X}_1 .